



LIGHTWEIGHT STRUCTURES in CIVIL ENGINEERING
CONTEMPORARY PROBLEMS
MONOGRAPH from INTERNATIONAL CONFERENCE
Organized by Polish Chapters of
International Association for Shell and Spatial Structures
Warsaw University of Technology, Faculty of Architecture
XX LSCE –2014
Warsaw, 25-28 September, 2014



The paper was reviewed by five members of Scientific Committee and accepted to printing by prof. dr hab. Jan B. Obrębski
(+/a , 10, 5.0, 5.0), (-/b , 9,3.66,4,5x), (+/c , 8, 4.0, 4.0), (+/a , 10, 5.0, 5.0), (na , xx, x, x, x)

Chapter 16

EXAMPLES OF ADVANCED ANALYSES FOR STRAIGHT BARS

J.B. Obrębski¹⁾

¹⁾ Retired Full Professor, Faculty of Civil Engineering, Warsaw University of Technology, POLAND

ABSTRACT: The paper gives short review of new elements of theories elaborated by present author, illustrated mainly by results of calculated examples presented in the previous author's publications. They permit to show unusual possibilities in domain of mechanics and strength analyses of structures formed as one separate bar, sometimes of large scale. The considered straight bars can be designed in many different ways. It can be homogenous and prismatic, or have complicated cross-sections - composed of some materials, dislocated in area of cross-section in many manners. Step by step are shown: foundation of the theory, some calculated results concerning of geometrical characteristics of bar cross-section, influence of bar torsion, determination of internal forces and stresses specially generated by torsion. The special attention is turned here on new derivations and examples of instability for such bars under action of combined state of external loadings, what lead to determination of ultimate critical curves or surfaces, shown in chapter 6. At last at the end of the paper is given information about analyses and shaping of complicated space bar structures, which can be built from many bars with, considered here internal structure. The list of references contains only the most important ones selected from 300. For wider lists, see to Refs 12, 21 and 23.

Keywords: straight bars, homogenous, composite cross-sections, analysis, stability, ultimate critical surfaces, combined loadings

1. INTRODUCTION

As it is announced in above abstract this paper is focused mainly on results of some comparative strength analysis of series of straight bars with composite and homogenous cross-sections built from steel and timber. In the beginning are shown by some drawings: scheme of the bar and system of loading, Fig. 1, considered cross-sections, Fig. 2 and then calculated internal forces, cores of cross-sections, positions of shearing centres (see chapter 3) and its influence on torsion moment and warping stresses. These examples and results were discussed in previous author's papers, Refs 17 to 21.

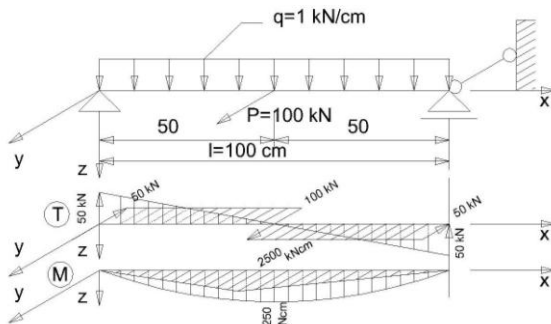


Fig. 1. Scheme of simply supported bar and internal forces.

Similarly, the way in chapter 6 presents the problem of instability of prismatic straight bars with length $l=400$ cm and with the same cross-sections shown in the Fig. 2. There, are given new elements of theory firstly given in book Ref. 6, next in some LSCE proceedings, Ref.23, and lately in papers Refs 24, 25. Essential part of these results is wide comparative one example, published in some mentioned above papers, of determination strength analysis and next of critical states of combined external loadings of three forces: longitudinal P acting with certain eccentricity and two bending moments M_2 and M_3 , applied along principal axes of main central coordinate system, Fig. 3.

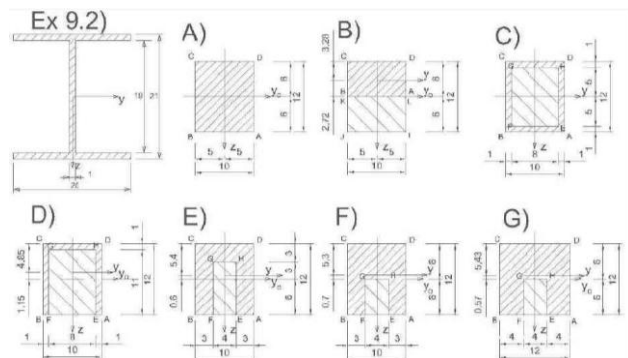


Fig. 2. Considered cross-sections built from steel and timber. Steel is shaded densely. Dimensions are given in [cm].

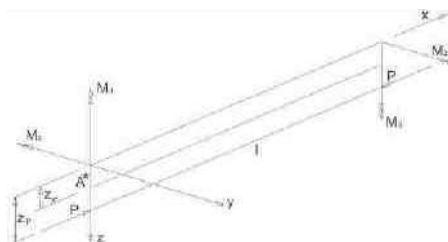


Fig. 3. Scheme of the mono-symmetrical bar loaded by eccentric longitudinal force P .

2. APPLIED THEORY

The wide elements of the theory elaborated by present author generally concern of the straight bars and structures composed from such elements:

- a) one straight bar or rather simple element of larger structure as subject of analyses, Refs 6, 9:
 - determination of geometrical characteristics of bar cross-section (cross-section of a bar rigidities),
 - determination of displacements,

- determination of internal forces in range of statics, dynamics, theory of first and second order, stability,
 - strength analysis - determination of stresses,
 - interaction of the bar with surrounding media, Refs 6,
- b) one bar as model of bridge or tall building (see Ref. 23 – own works, and dissertation of R. Szmit),
- c) complicated large space bar structures Refs 2-4,

The review of theories, subjects, tasks, numerical examples and experimental works were published in wide papers Refs 12, 15, 20, 21, 24. Number of scientific publications of different type written by the present author is exactly 300 (including year 2014 & not counting supervised M.Sc. and Ph.D. dissertations and other type papers). Relatively wide lists of author's works are given in Refs 12, 21 and 23.

This paper is concentrated on subject, especially intensive investigated in last year's, on strength analyses and instability of the straight bars with any type of cross-sections, including composite - built from a few different materials, Refs 6, 7, 15-25. There, is applied uniform criterion published by author first time in 1997, Refs 8, 13, 16. Especially in Refs 22 and in present, are done some extensions of theory from book Ref 6.

So, in Ref. 22 are derived formulae for calculation of critical loadings for composite bar with mono-symmetrical cross-section under combined external loading, longitudinal compressing force and moment bending the bar in plane of its symmetry. Now it is repeated derivation for compressing longitudinal force and two bending moments applied in two principal planes of the cross-section, Fig. 3 and chapter 6.2.

In the past, the examples of instability of the bar under combined loading were published with J. Tolksdorf, Ref. 10, 11.

3. GEOMETRICAL CHARACTERISTICS OF BARS CROSS-SECTIONS

There, key-matter to any analyses of single bar and even whole large space bar structure is definition of so called reduced geometrical characteristics for cross-sections, Refs 5, 7, 9, and 17. As the first such characteristics is defined reduced area of the bar cross-section:

$$\bar{A} = \int d\bar{A}, \quad d\bar{A} = \left(\frac{E_1}{E}\right) \delta ds = \left(\frac{E_1}{E} \delta\right) ds = \bar{\delta} ds, \quad (1)$$

where, is introduced reduced elementary area $d\bar{A}$ (or for thin-walled cross-section a thicknesses of the bars walls):

$$\bar{\delta} = \left(\frac{E_1}{E} \delta\right).$$

So defined reduced area of composite cross-section is an element for calculation of next, remaining reduced geometrical characteristics, such as e.g. reduced moments of inertia, in it "sectorial moments of inertia" necessary for taking into consideration torsion of the bars and general effects of instability with bending-torsion character, up to now omitted – not possible in other theories and first of all in standards and in contemporary designing process. Examples of definitions of reduced moments of inertia, in it sectorial, are given below:

$$\bar{I}_i = \int (\eta_j)^2 d\bar{A}, \quad i, j=2, 3 \wedge i \neq j, \quad (2)$$

$$\bar{I}_{23} = \int \eta_2 \eta_3 d\bar{A}, \quad \bar{I}_{\hat{\omega}} = \int (\hat{\omega})^2 d\bar{A}, \quad \bar{I}_{j\hat{\omega}} = \int \eta_j \hat{\omega} d\bar{A}, \quad j=2,3.$$

Further definitions of the geometrical characteristics following of interaction the bar with surrounding media and so called „mass-characteristics” (Ref. 5) necessary for dynamical analysis, are presented in the books Refs 6, 9.

In this theory are defined “reduced principal axes” of the cross-section, for which are equal zero some geometrical characteristics (static moments and proper centrifugal moments of inertia – all reduced):

$$\bar{S}_2 = \bar{S}_3 = \bar{S}_{\hat{\omega}} = \bar{I}_{23} = \bar{I}_{2\hat{\omega}} = \bar{I}_{3\hat{\omega}} = 0. \quad (3)$$

3.1. Core of cross-section

For each cross-section as the first was calculated reduced centre of gravity (Fig. 4, axis y), by means of special authors program MBK facilitating calculations.

Calculated shapes of cross-sections cores are shown in the Fig. 4. They were determined according to following formulae, (Obrębski, Refs 17, 18 and 24):

$$z_0 = -\frac{\bar{I}_2}{e_3}, \quad y_0 = -\frac{\bar{I}_3}{e_2} \quad \& \quad \bar{I}_2^{-2} = \frac{\bar{I}_2}{A}, \quad \bar{I}_3^{-2} = \frac{\bar{I}_3}{A}, \quad (4)$$

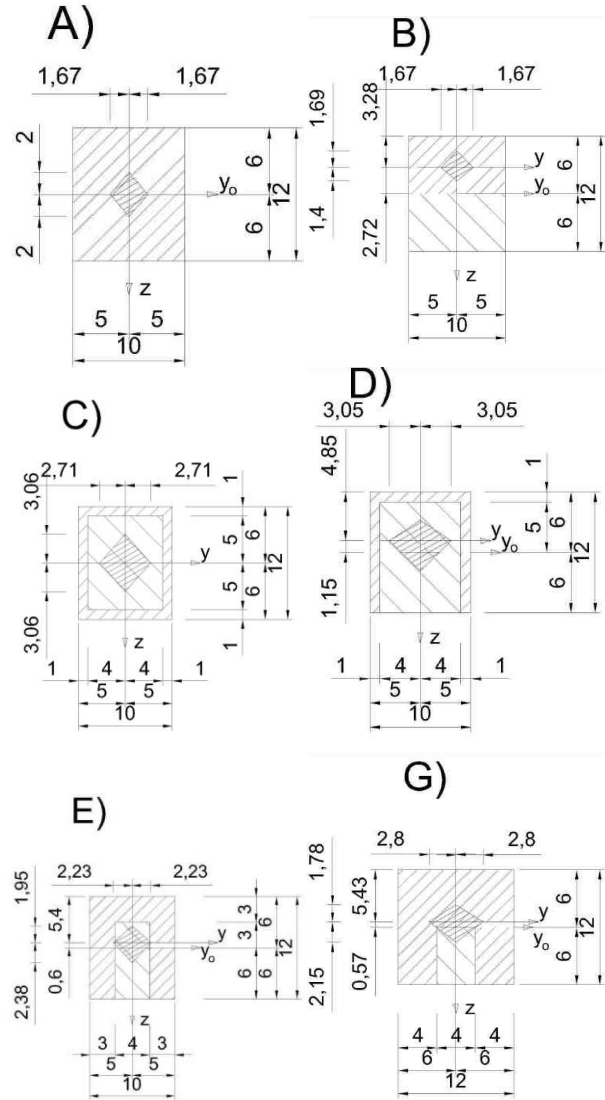


Fig. 4. Cores determined for considered full composite cross-sections. Dimensions are given in [cm].

3.2. Warping of cross-section

For the beams with scheme given in the Fig.1 and with cross-sections shown in the Fig.2, were applied two kinds of division on closed tubes. In the case indicated by letters Xa) were applied only rectangular thin-walled tubes with thickness of walls 1cm – homogenous or composite (at down sector of timber). In the cases Xb) were applied only closed homogenous tubes made of steel or timber, what is visible in the Fig. 3 (Obrębski, Refs 18, 19).

For each such tube were calculated in the beginning warping functions with pole in origin of reduced principal coordinates of the cross-section, next shearing centre and in last final shapes of warping function for each thin-walled tube. So, the cross-section under action of bar loading,

especially torsion, appears as complicated surface with indifferent curves (set of points not moving along the bar).

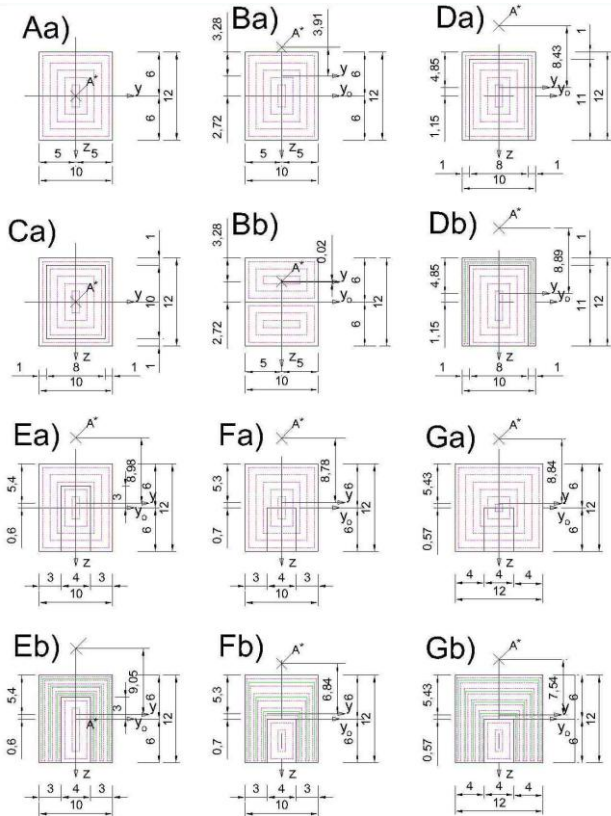


Fig. 5. Applied division of the cross-sections on tubes of type I to IV, see Refs 19 22. Visible axes and position of shearing centres A^* .

3.3. Geometrical characteristics associated with warping of cross-section

Values of reduced geometrical characteristics for all considered cross-sections depend on assumed comparative Young's reduced modulus \bar{E} assumed for whole composite cross-section, and Young's modulus for materials build into it Refs 6, 9. The results of such calculations for the cross-sections shown in the Fig.2 are given in some last works, Refs 17, 18, 20, and 21.

Especially important part in mechanical behaviour of the bars play warping function $\hat{\omega}(s)$ (calculated for closed tubes) or $\omega(s)$ (calculated for open tubes), see Refs 6, 9. On the ground of this function, are determined next "reduced sectorial" geometrical characteristics (see Eqns 2): $\bar{S}_{\hat{\omega}}$, $\bar{I}_{\hat{\omega}}$, $\bar{I}_{2\hat{\omega}}$, $\bar{I}_{3\hat{\omega}}$. They are very important for calculation of critical combined loadings of bars with any type of cross-sections.

3.4. Shearing centre

As it was shown in the chapter 3.2 and in the Fig. 5, the full cross-section, even composite as in the Fig.2 (or reinforced concrete), can be regarded as set of thin-walled tubes filling it. Such division can be done on many ways, but each time it answers to a little other structural solution and then behaviour of the whole bar. The cross-sections from Fig. 2 were comparatively divided on closed tubes, only, but in two manners (see chapter 3.2 and Fig. 5). In effect in each case were obtained a little other result.

For beams modelled in this way, were performed comparative strength analyses. Calculated positions of shearing centres (A^*) are shown in the Fig.3 (Obrębski, Ref 18, 19). The calculated these way positions of shearing centres for each type of CS are defined by two coordinates:

$$\eta_{2A^*} = \frac{\bar{I}_{3\hat{\omega}}}{\bar{I}_2} \quad , \quad \eta_{3A^*} = \frac{\bar{I}_{2\hat{\omega}}}{\bar{I}_3} \quad . \quad (5)$$

3.5. Geometrical characteristics associated with interaction of bar with surrounding media

In the author's Ref 5 and book Ref 6 was possible analysis of thin-walled bars having contact with surrounding media: gas (e.g. air), liquid (e.g. water) and soil. Derived there formulae and equations are valid for full cross-sections if we remember only, that contact with surrounding media have only external tubes modelling the bar, Ref. 9. So, such these geometrical characteristics depend on shape of cross-section. Examples of calculations of such type geometrical characteristics were done in the author's books 6, 9, and in the works published with R. Szmit and in his Ph.D. dissertation concerning of dynamics of tall buildings (see Refs 12, 23).

3.6. Geometrical characteristics associated with mass of cross-section

For dynamical behaviour of straight bars were derived special set of four differential equations of motion of fourth order, according to theory of second order, containing "inertial (mass) geometrical characteristics" - other from ordinary e.g. moments of inertia. They contain density of materials, see Refs 5, 6. Given their definition are valid for any type cross-sections as thin-walled, full and composite - all modelled as sets of thin-walled (composite) tubes (or open type) located one into the other. Examples of calculation such inertial geometrical characteristics are given in the Refs 6, 23 and in mentioned in chapter 3.5 works with R.Szmit devoted (oriented) on dynamics of tall buildings.

4. INTERNAL FORCES

Internal forces associated with torsion, such as bimoment and bending-torsion moment (Fig.5), were calculated for considered bars shown in the Figs 1, 2, 3, according to formulae used in theory of thin-walled bars, see Obrębski, Ref 6. Results of calculation are given in the Fig.6. There M_w means bending-torsion moment (M_{ω} -see e.g. Refs 5, 6, 9). Calculation of these internal forces is up to now not applied for bars with full cross-section. It starts to be possible after modelling the bar as set of tubes located each into the other.

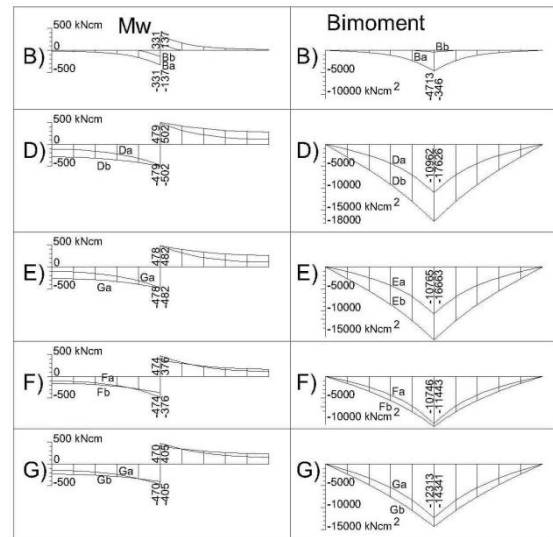


Fig. 6. Diagrams of internal forces calculated for bar shown in the Fig. 1 with full composite CSs from the Fig. 2. In all cases are obtained strong values of torsion-bending moments (at left) and bimoment (at right). On each diagram are shown two curves for two manners of CS division, shown in the Fig. 5.

5. STRENGTH ANALYSIS OF STRAIGHT BARS

Strength analysis for the composite prismatic bars with composite cross-sections is led in such a way, that:

- sectorial moments of inertia for whole cross-section is calculated as algebraic sum of all thin-walled tubes consisting on bar,
- bimoment B and bending-torsion moment M_{ω} are determined for whole bar,
- warping (sectorial) function $\hat{\omega}$ and sectorial statical moment $\bar{S}_{\hat{\omega}}$ are

calculated separately for each thin-walled tube, but with one common shearing centre A^* , - stresses are calculated for all thin-walled tubes.

5.1. Normal stresses

Normal stresses were calculated according to Eqn. 6. Proper results are given in the Figs 7 and 8.

$$\sigma_1 = \frac{E_1}{E} \left(\frac{T_1}{A} - \frac{M_3 \eta_2}{I_3} + \frac{M_2 \eta_3}{I_2} + \frac{B \hat{\omega}}{I_{\hat{\omega}}} \right) \quad (6)$$

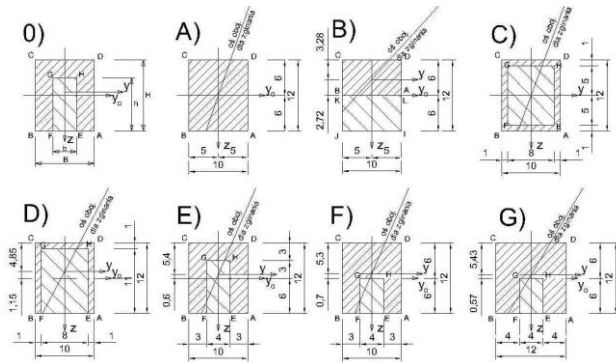


Fig. 7. Considered cross-sections. It is visible inclination of indifferent axes, when torsion is omitted (last term in Eqn.6).

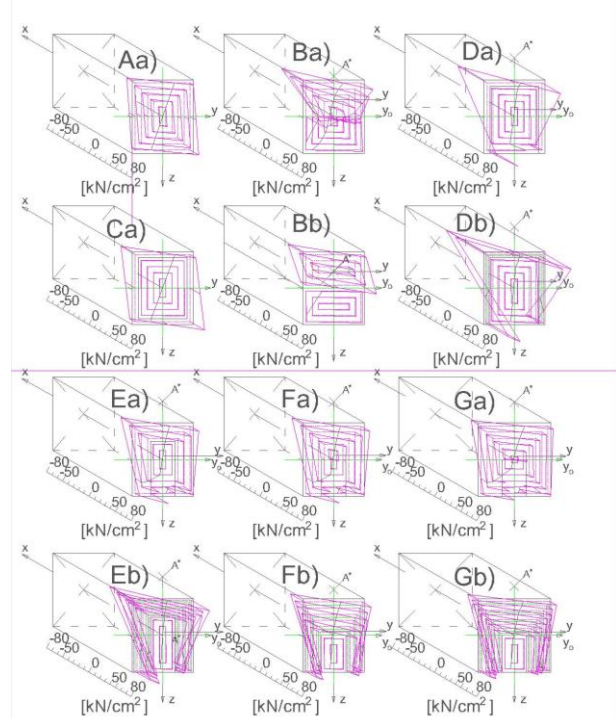


Fig. 8. Normal stresses calculated by means of Eqn. 6 for particular full composite CSs and for each tube.

If we compare especially normal stresses shown in the Figs 7 & 8, there are visible evidently high differences concerning as well shape of diagrams and values of calculated stresses. The indifferent axis well known in traditional strength calculations as straight line (see Fig.7, it is inclined differently for each type cross-section), when torsion is taken under consideration, appears as curved line! If torsion does not exist, (CSs A & C) it stays the straight line...

5.2. Shearing stresses

Shearing stresses were calculated according to Eqn 7. Proper results are given in the Fig 9 (with torsion).

$$\tau_{1s} = \tau_o - \frac{1}{\delta} \left(\frac{T_2 \tilde{S}_3}{I_3} + \frac{T_3 \tilde{S}_2}{I_2} + \frac{M_{\hat{\omega}} \tilde{S}_{\hat{\omega}}}{I_{\hat{\omega}}} \right) \quad (7)$$

5.3. Part of torsion in calculated stresses

Warping stresses in many tasks obtain significant values, what for two examples presented in author's book Ref. 6 and in Figs 10 and 11.

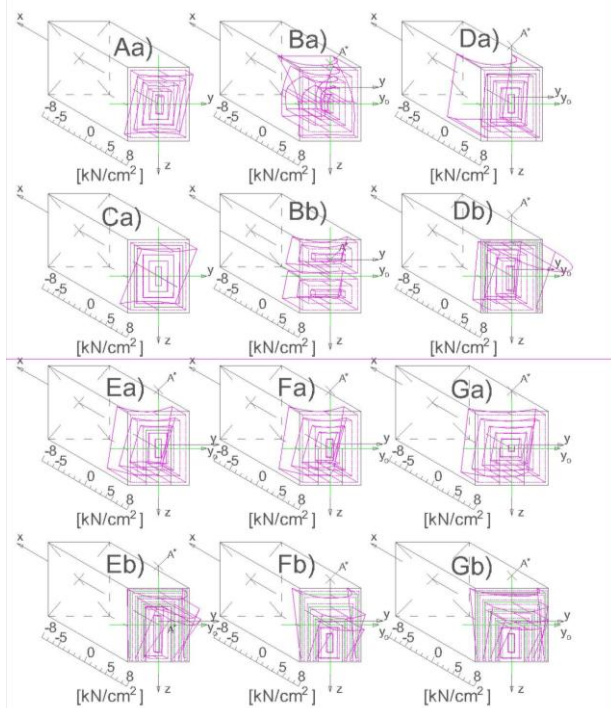


Fig. 9. Shearing stresses calculated for particular full composite CSs and for each tube.

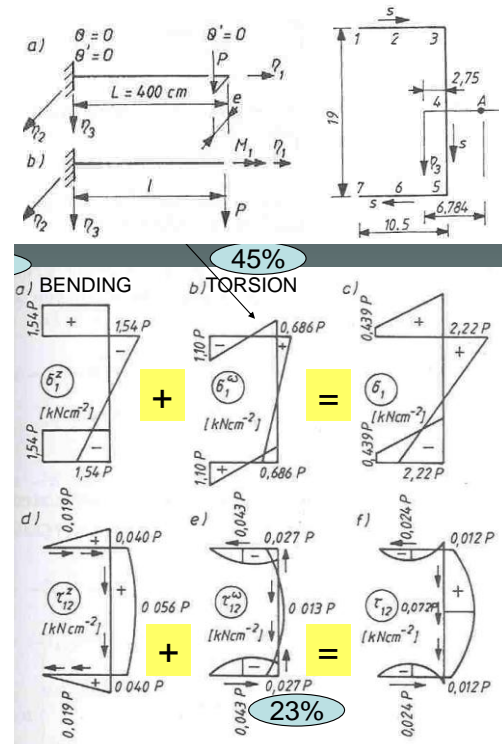


Fig. 10. Normal stresses in upper row and shearing stresses in lower row, calculated for cantilever beam and with channel CSs with dimensions 10.5×19 cm. Normal warping stresses have 45% input with regard to bending (upper row). Similarly shearing stresses gives 23% input (lower row).

Simultaneously, it should be compared e.g. normal stresses calculated for simply supported beam when omitted torsion, see Fig 7 and when effect of torsion is added, see Fig 8. Their differences are radical.

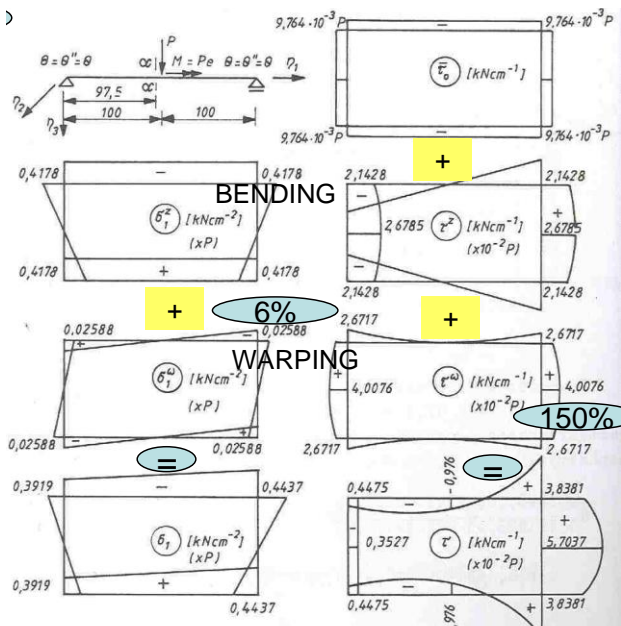


Fig. 11. Normal stresses in left column and shearing stresses in right column, calculated for simply supported beam and with closed box CSs with dimensions 20×10 cm. Normal warping stresses have 6% input with regard to bending. Similarly shearing warping stresses gives 150% input.

5.3. Comments to strength analyses of composite bars

Strength analysis of the bars depends on many structural solutions:

- bar length, its boundary conditions for each of function describing independently displacements of bar axis, type of applied cross-section, position of shearing centre, external bar loading,
- position of shearing centre and magnitude and shape of cross-section core depend not only on shape of cross-section, but also on dislocation and strength of applied materials,
- cross-section of the bar under torsion has very complicated shape of stresses and there indifferent "axis" is not straight, but curved line,
- change of type cross-section generates changes of:

- bar rigidity including torsion rigidity K_s ,

$$K_s = \sum_{i=1}^N \frac{(\Omega_i)^2 G_i \delta_i}{L_i} = \sum_{i=1}^N K_{s_i}$$

- sectorial moment of inertia \bar{I}_ω ,
- shape of its warping function (deplanation - sectorial coordinates),

- thin-walled cross-section assures very well structural behaviour of the bar.

6. INSTABILITY OF BARS

Problem of bars instability is much more complicated, than it is widely applied in nowadays engineers practice. It is really multi-parametrical task, Refs 8, 13, 24. In last papers present author has investigated critical states of combined loadings of bar from Fig. 3 with series of mono-symmetrical cross-sections given in the Fig. 2. In effect were obtained using so called "uniform criterion" (see chapter 6.1) ultimate critical curves, Refs. 22, 24, 25. There, were derived proper formulae for calculation of critical compressing forces or/and critical bending moment.

Below, is given derivation of set of formulae helpful for calculation of this time ultimate critical surfaces for combined external loadings: compressing eccentric longitudinal force and two bending moments applied along two principal central axes of bar cross-section. Next, are shown three examples of such critical surfaces determined for three cross-sections: type A, C and Ex 9.2 all showed in the Fig. 2.

6.1. Uniform criterion and instability of bars

The uniform criterion for determination of critical states of external loadings was formulated by Obrębski in 1997 Ref. 8 and next extended

for further applications Refs 12, 13, 16 Some conference papers were published with J. Tolksdorf, too Refs. 10, 11. Certain summary of the criterion application and wide list of author's references is given in the papers written by Obrębski Ref 12 and 18 to 24. In the most general form the criterion of instability of the structure can be expressed as follow:

$$\text{Det [K(P, } \omega, \nu, a, M, m, d, t)] = 0 \quad (8)$$

where particular arguments means: system of forces, frequency of free vibrations, loading velocity, acceleration of loading, moving mass, mass of structure, dumping effects, time etc. As next can be pointed various boundary conditions, internal structure of e.g. bar. The stiffness matrix K in above condition can be obtained in some ways: analytically - as by Euler, Vlasov etc., or by means of FEM or FDM, too.

6.2. Applied equations for calculated critical states

Theoretical solution was started on the ground of four very large equations of second and fourth order (see Ref. 6, Eqns (9.26)) taking into consideration theory of second-order, external loadings, boundary conditions and second order effects. In a little changed form, omitting the first equation (influence of longitudinal continuous loadings) and dropping some small quantities, similarly as in Ref. 22 some small quantities, was obtained much shorter version of considered equations (Ref. 22, page 87 Eqns 6):

$$2) \quad \bar{E} I_3 v_2'' - N v_2 + Q_2 + (M_2 - N \eta_{3A}) \Theta = M_3, \quad (9)$$

$$3) \quad \bar{E} I_2 v_3'' - N v_3 + Q_3 + (M_3 + N \eta_{2A}) \Theta = -M_2, \\ \bar{E} I_\omega \Theta'' - K_s \Theta''$$

$$4) \quad -\Theta \int [p_3(\eta_{3A} - \eta_3) + p_2(\eta_{2A} - \eta_2)] ds + \\ + [M_2 + Q_3 - N \eta_{3A}] v_2'' + \\ + [M_3 - Q_2 + N \eta_{2A}] v_3'' + \\ - [\Theta' (T_1 r^2 - 2\beta_2 M_3 + 2\beta_3 M_2 + 2\beta_\omega B)]' - b' - m_1 = 0$$

In above equations is used following notation (see Ref 6, pp. 42, 76, 77 and Ref. 22, page 87):

\bar{E} - Young's reduced modulus assumed for whole composite cross-section,

\bar{A} - reduced area of bar cross-section,

\bar{I}_2, \bar{I}_3 - reduced moments of inertia for transversal cross-section of the bar, with regard relatively to principal its axes η_2 and η_3 ,

\bar{I}_ω - reduced sectorial moment of inertia of the cross-section,

T_1, M_2, M_3, B - internal, cross-sectional forces: longitudinal, bending moments with regard to axes η_2 and η_3 , and bimoment - calculated in undeformed configuration of the bar,

τ_p, τ_l - given shearing stresses on right and left longitudinal bar edges,

N - longitudinal tensioning force acting on the ends of whole bar (see Ref. 3, page 233, Eqn (9.29)),


v_1, v_2, v_3, Θ - displacements of the line formed by of bar cross-sections main poles (parallel to three bar principal axes η_i and rotation with regard to above longitudinal line),


p_i - real continuous loading acting in each point of bar walls (its middle surface) $[N/cm^2]$ parallel to axes of general bar coordinates η_i ,

η_{2A}, η_{3A} - coordinates of main pole for bar cross-section (in theory of first order equivalent to shearing centre).

Moreover it can be calculated according to Ref. 6:

$$q_b = \int p_i ds \quad - \text{continuous loading acting on longitudinal unit of the bar section } [N/cm],$$

 - continuous torsion moment acting on longitudinal unit of the bar section (see Ref 6, Eqn (7.1), Fig 7.1, page 143),

 - continuous external bimoment (acting on longitudinal unit of the bar section (see Ref. 6, Eqn (3.57a), page 62).

Besides of above, are defined:

➤ torsion rigidity of the bar of cross-section (Ref. 6, Eqn (4.5), page 72 and Eqn (4.13) page 76):

$$K_s = K_o + K_z = \beta \sum_{i=1}^n I_s^i G_i + \left(\int \frac{c^2 ds}{G\delta} \right)^{-1} = \beta \frac{1}{3} \sum_{i=1}^n G_i b_i \delta_i^3 + \frac{1}{\int \frac{c^2 ds}{G\delta}} \quad (10)$$

➤ and other auxiliary magnitudes are defined in following way:

$$r^2 = \frac{\bar{I}_A}{A} \quad (\text{Ref 6, page 230}) \text{ or } \frac{2}{A} \int \frac{E \bar{I}_s}{A} ds \quad (11)$$

$$\bar{I}_A = \int \beta^2 d\bar{A}$$

next (Ref 6, Eqns (9.22) to (9.25), page 231):

$$\begin{aligned} \beta_2 &= \frac{1}{2I_3} \left[\int (\eta_2)^3 d\bar{A} + \int (\eta_3)^2 \eta_2 d\bar{A} \right] - \eta_{2A} \\ \beta_3 &= \frac{1}{2I_2} \left[\int (\eta_3)^3 d\bar{A} + \int (\eta_2)^2 \eta_3 d\bar{A} \right] - \eta_{3A} \\ \beta_{\bar{\omega}} &= \frac{1}{2I_{\bar{\omega}}} \left[\int (\eta_2)^2 \bar{\omega} d\bar{A} + \int (\eta_3)^2 \bar{\omega} d\bar{A} \right] \end{aligned} \quad (12)$$

If we assume, that longitudinal force is compressing the bar $P = -N$ and $q_1 = 0$ (longitudinal uniform loading), three our Eqns 9, can be written as below (Ref. 22 & Eqn 13):

$$\begin{aligned} 2) \quad & \bar{E}I_3 v_2'' + P v_2 + (M_2 + P \eta_{3A}) \Theta = M_3, \\ 3) \quad & \bar{E}I_2 v_3'' + P v_3 + (M_3 - P \eta_{2A}) \Theta = -M_2, \\ 4) \quad & [M_2 + P \eta_{3A}] v_2'' + [M_3 - P \eta_{2A}] v_3'' + \bar{E}I_{\bar{\omega}} \Theta'' - K_s \Theta'' - \\ & - \Theta \int [p_3(\eta_{3A} - \eta_3) + p_2(\eta_{2A} - \eta_2)] ds + \\ & - [\Theta'(T_1 r^2 - 2\beta_2 M_3 + 2\beta_3 M_2 + 2\beta_{\bar{\omega}} B)]' - b' - m_1 = 0 \end{aligned} \quad (13)$$

Moreover, for our task, Eqns 13 can be written much shortly (Ref. 22, Eqn 8):

$$\begin{aligned} 2) \quad & \bar{E}I_3 v_2'' + P v_2 + d_1 \Theta = M_3, \\ 3) \quad & \bar{E}I_2 v_3'' + P v_3 + d_2 \Theta = -M_2, \\ 4) \quad & d_1 v_2'' + d_2 v_3'' + \bar{E}I_{\bar{\omega}} \Theta'' - (K_s + g) \Theta'' - g' \Theta' = 0 \end{aligned} \quad (14)$$

when is introduced notation (Ref 6, Eqns (9.38) & Ref. 22 Eqn 8):

$$\begin{aligned} d_1 &= M_2 + P \eta_{3A}; \quad d_2 = M_3 - P \eta_{2A}; \\ g &= -P r^2 - 2\beta_2 M_3 + 2\beta_3 M_2 + 2\beta_{\bar{\omega}} B \end{aligned} \quad (15)$$

Next, we introduce for solution of Eqns 14 following three functions for displacements of bar axis, when $n=1$ (first critical force and bar is simply supported) filling of boundary conditions:

$$\begin{aligned} \Theta &= C_1 \sin(a_1 \alpha_n \eta) = C_1 \sin\left(a_1 \frac{n\pi}{l} \eta\right), \\ v_2 &= C_2 \sin(a_2 \alpha_n \eta) = C_2 \sin\left(a_2 \frac{n\pi}{l} \eta\right), \\ v_3 &= C_3 \sin(a_3 \alpha_n \eta) = C_3 \sin\left(a_3 \frac{n\pi}{l} \eta\right). \end{aligned} \quad (16)$$

It is easily to proof, that above functions for bar with length l on its ends: for $\eta = 0$ and for $\eta = l$ are giving zero values when in above functions are applied following values of used three coefficients:

- a) for simply supported beam $a_i = 1$ and $A_i = (a_i)^2 = 1$,
b) for cantilever $a_i = 0.5$ and $A_i = (a_i)^2 = 0.25$ there, task is solved as for bar with double length - fixed in the middle.

So, these coefficients a_i and A_i describe bar boundary conditions (see Ref. 6, Table 9.2, page 237), and are identical as in widely applied generalized Euler's solutions for simply supported beam.

Now, we put relations 16 to Eqns 14 with application notation of so written two traditional Euler's critical forces for both above cases a) and b), (Eqn (9.42), Ref 6) given here in following way:

$$P_2 = EI_2 A_3 \alpha_n^2 = A_3 \frac{EI_2 n^2 \pi^2}{l^2} = A_3 \frac{EI_2 \pi^2}{l^2}, \quad (17)$$

$$P_3 = EI_3 A_2 \alpha_n^2 = A_2 \frac{EI_3 n^2 \pi^2}{l^2} = A_2 \frac{EI_3 \pi^2}{l^2}.$$

By analogy additionally is introduced here

$$P_{\bar{\omega}} = EI_{\bar{\omega}} A_1 \alpha_n^2 = A_1 \frac{EI_{\bar{\omega}} n^2 \pi^2}{l^2} = A_1 \frac{EI_{\bar{\omega}} \pi^2}{l^2} \quad (18)$$

where $\alpha_n = \frac{n\pi}{l}$ and $n=1$ (first critical force).

By such notation torsion Wagner's critical force Eqn 19, has form:

$$\bar{P}_{\bar{\omega}} = \frac{1}{r^2} (P_{\bar{\omega}} - 2\beta_2 M_3 + 2\beta_3 M_2 + 2\beta_{\bar{\omega}} B) \quad (19)$$

where $P_{\bar{\omega}} = \bar{E}I_{\bar{\omega}} A_1 \alpha_n^2 + K_s = P_{\bar{\omega}} + K_s$,

or

$$\bar{P}_{\bar{\omega}} = \frac{1}{r^2} (P_{\bar{\omega}} + K_s - 2\beta_2 M_3 + 2\beta_3 M_2 + 2\beta_{\bar{\omega}} B) \quad (20)$$

After all last operations with introduced notation, finally we come to following form of uniform criterion on instability of the bar (see Refs 6, Eqn (9.45) and Refs. 8, 9, 10, 22, 24, 25):

$$W(P) = \det \begin{bmatrix} (P - P_3) & 0 & d_1 \\ 0 & (P - P_2) & d_2 \\ A_2 d_1 & A_3 d_2 & -A_1 r^2 (\bar{P}_{\bar{\omega}} - P) \end{bmatrix} = 0 \quad (21)$$

Now, we extend formulae expressed by Eqns 15 to following shape:

$$d_1 = M_2 + P \eta_{3A} = \bar{M}_2 - P \eta_{3P} + P \eta_{3A} = \bar{M}_2 + P(\eta_{3A} - \eta_{3P}), \quad (22)$$

$$d_2 = M_3 - P \eta_{2A} = \bar{M}_3 + P \eta_{2P} - P \eta_{2A} = \bar{M}_3 + P(\eta_{2P} - \eta_{2A}).$$

In above both definitions it was additionally taken, that:

$$M_2 = \bar{M}_2 - P \eta_{3P}, \quad M_3 = \bar{M}_3 + P \eta_{2P}.$$

It means, that bending moments in cross-section are the sums of given moments (with head bars) and part generated by longitudinal eccentric (with regard to principal reduced axes η_{2P} and η_{3P}) compressing force P .

Moreover, for bisymmetrical cross-sections relations expressed by Eqns 12 disappear:

$$\beta_2 = \beta_3 = \beta_{\bar{\omega}} = 0,$$

and then the torsion Wagner's critical force Eqn 19 has obtain shorter form:

$$\bar{P}_{\bar{\omega}} = \frac{1}{r^2} (P_{\bar{\omega}} + K_s).$$

In this way condition (21) can be written as function of three external forces in following manner:

$$\begin{aligned} W(P, M_2, M_3) &= A_1 r^2 (P - P_2)(P - P_3)(P - \bar{P}_{\bar{\omega}}) + \\ &- A_2 (P - P_2)(M_2)^2 - A_3 (P - P_3)(M_3)^2 = 0 \end{aligned} \quad (23)$$

or finally for bar compressed by longitudinal force and bended by two moments, as it is shown in the Fig. 3, we have:

$$W(P, M_2, M_3) = D_1 + D_2 (M_2)^2 + D_3 (M_3)^2 = 0, \quad (24)$$

where:

$$D_1 = A_1 r^2 (P - P_2)(P - P_3)(P - \bar{P}_{\bar{\omega}}), \quad (25)$$

$$D_2 = -A_2(P - P_2), \quad D_3 = -A_3(P - P_3)$$

On the other hand Eqn 23 can be expressed in following form:

$$W(P, M_2, M_3) = (P - P_2)(P - P_3)(P - \bar{P}_\omega) - \frac{A_2(P - P_2)}{A_1 r^2} (M_2)^2 + \frac{A_3(P - P_3)}{A_1 r^2} (M_3)^2 = 0 \quad (26)$$

Moreover, denoting:

$$K = \frac{A_2(M_2)^2}{A_1 r^2} \quad \text{and} \quad L = \frac{A_3(M_3)^2}{A_1 r^2}, \quad (27)$$

the Eqn 26 can be written in the following form:

$$W(P, M_2, M_3) = (P - P_2)(P - P_3)(P - \bar{P}_\omega) - K(P - P_2) - L(P - P_3) = 0, \quad (28)$$

By means of condition Eqn 28 are solved all announced tasks. However in some calculations were used special cases of the Eqn 25, given below.

Case, when both bending moments are given.

This is general case. After some simple modifications from Eqn 28 we obtain:

$$W(P, M_2, M_3) = P^3 + P^2 C_1 + P C_2 + C_3 = 0 \quad (29)$$

here is given new notation:

$$\begin{aligned} C_1 &= -(P_2 + P_3 + \bar{P}_\omega) \cdot \\ C_2 &= (P_2 + P_3)\bar{P}_\omega + P_2 P_3 - K - L \cdot \\ C_3 &= K P_2 + L P_3 - P_2 P_3 \bar{P}_\omega \cdot \end{aligned}$$

From Eqn 29 by given values of bending moments, we can obtain critical value of compressing force P. It is equation of third grade. Its solution manually is not convenient and needs application rather computer.

Case, when bending moments are absent $M_2=M_3=0$.

In this case from Eqn 24 follow simple condition:

$$W(P) = D_1 = 0 \quad (30)$$

or applying Eqn. 25 above condition has the form:

$$D_1 = A_1 r^2 (P - P_2)(P - P_3)(P - \bar{P}_\omega) = 0 \cdot$$

Finally from Eqn 30 we obtain condition on value of critical force

$$f(P) = (P - P_2)(P - P_3)(P - \bar{P}_\omega) = 0 \quad (31)$$

Above equation is fulfilled by three roots:

$$\bar{P}_1 = P_2, \quad \bar{P}_2 = P_3, \quad \bar{P}_3 = \bar{P}_\omega \cdot$$

The smallest of the above roots is the critical force, see Fig. 12. These calculations are easy. This way were determined the highest points of surfaces of the Figs 13, 19, 31 and for some of presented critical curves given in the Figs given below (when they are symmetrical).

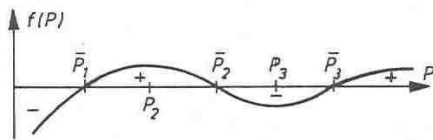


Fig. 12. Three roots of Eqn 28.

Case when M_2 and force P are given.

From Eqn 24 is obtained following relation, useful for determination of characteristic points of contour lines for vertical sections of ultimate critical surfaces:

$$M_3 = \pm \sqrt{\frac{-D_1}{D_3} - \frac{(M_2)^2 D_2}{D_3}} \quad kNcm \quad (32)$$

Particular case of Eqn 27 when $M_2=0$ and force P is given

$$M_3 = \pm \sqrt{\frac{-D_1}{D_3}} = \pm r \sqrt{(P - P_2)(P - \bar{P}_\omega) \frac{A_1}{A_3}} \quad kNcm \quad (33)$$

Particular case of Eqn 27 when $M_2=P=0$ are given

$$M_3 = \pm \sqrt{\frac{-D_1}{D_3}} = \pm r \sqrt{P_2 \bar{P}_\omega \frac{A_1}{A_3}} \quad kNcm \quad (34)$$

Case when M_3 and force P are given.

From Eqn 24 is obtained following relation, useful for determination of characteristic points of contour lines for vertical sections of ultimate critical surfaces:

$$M_2 = \pm \sqrt{\frac{-D_1}{D_2} - \frac{(M_3)^2 D_3}{D_2}} \quad kNcm \quad (35)$$

Particular case of Eqn 30 when $M_3=0$ and force P is given.

$$M_2 = \pm \sqrt{\frac{-D_1}{D_2}} = \pm r \sqrt{(P - P_3)(P - \bar{P}_\omega) \frac{A_1}{A_2}} \quad kNcm \quad (36)$$

Particular case of Eqn 30 when $M_3=P=0$ are given.

$$M_2 = \pm \sqrt{\frac{-D_1}{D_2}} = \pm r \sqrt{P_3 \bar{P}_\omega \frac{A_1}{A_2}} \quad kNcm \quad (37)$$

6.3. Examples of ultimate critical curves and surfaces for combined bar loading

Applying uniform criterion and derived above formulae, were determined critical combined loadings for bars with scheme given in the Fig. 3 considered with seven cross-sections from the Fig. 2, containing two materials: steel and timber. Additionally was calculated example of homogenous steel cross-section Ex 9.2, Fig. 2, taken from book written by Obrębski (Ref. 6).

The results of comparative calculations for series of seven bars with the same length $l=400$ cm, were presented partially in papers of Obrębski, Refs 22, 24, 25. Now, these information are completed by contour lines of ultimate critical surfaces ($P=\text{const.}$, $M_2=\text{const.}$, $M_3=\text{const.}$) and diagrams of ultimate instability surfaces for combined loadings, given in the Figs 13, 19 and 31. Safe zones are below the curves or inside (here below) of shown surfaces. Points on the curves or surfaces mean instability – critical state.

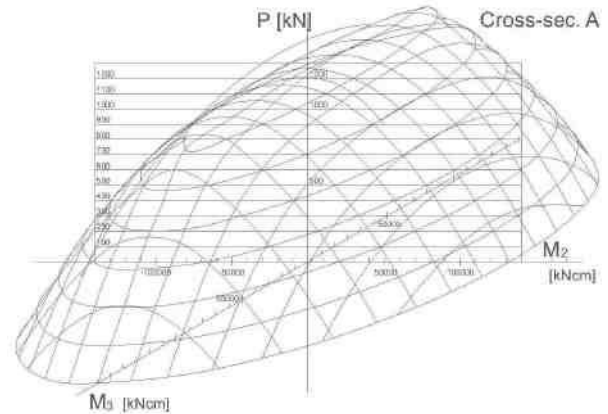


Fig. 13. Example of ultimate critical surface for combined loadings: P, M_2 and M_3 for cross-section A. Simply supported beam. Force P is acting in origin of coordinates.

By preparation of mentioned and shown below diagrams, were used values:

$$\begin{aligned} P &= 0, 100, 200, 300 \text{ up to } 1800 \text{ kN}; \\ M_2 &= 0, \pm 10000, \pm 20000, \pm 40000, \dots, \text{ up to } \pm 140000 \text{ kNcm}, \\ M_3 &= 0, \pm 10000, \pm 20000, \pm 40000, \dots, \text{ up to } \pm 160000 \text{ kNcm}, \end{aligned}$$

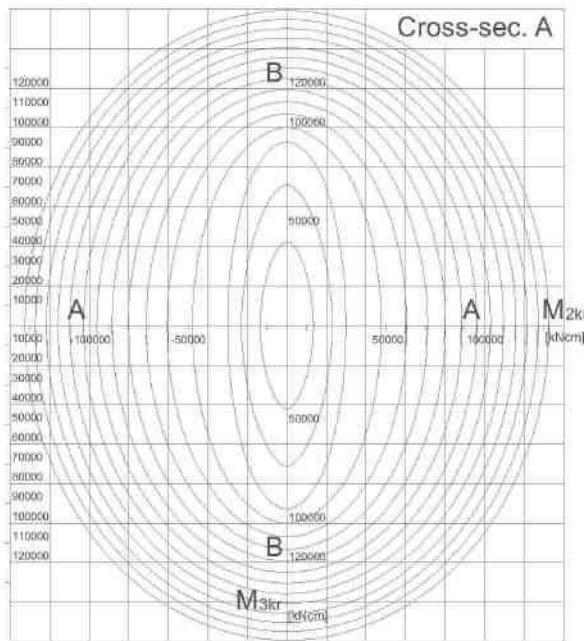


Fig. 14. Contour lines on ultimate critical surface for given forces P, cross-section A, (Fig. 13). Force P is acting in origin of coordinates.

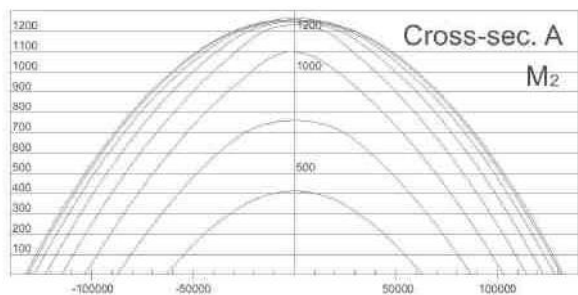


Fig. 15. Contour lines on ultimate critical surface for combined loadings P and M_2 for cross-section A (M_3 is given), Fig. 13 [22].

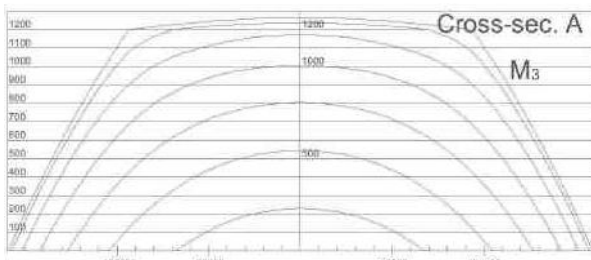


Fig. 16. Contour lines on ultimate critical surface for cross-section A when M_2 is given, (Fig. 13). Force P is acting in origin of coordinates.

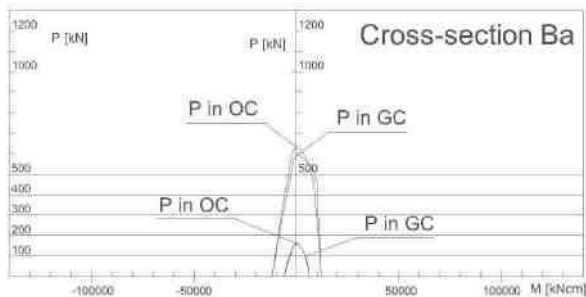


Fig. 17. Contour lines for cross-section Ba when $M_3=0$. Upper lines for simply supported beam and lower for cantilever. Moreover, longitudinal force is acting in geometrical centre (GC) or in origin of coordinates (OC).

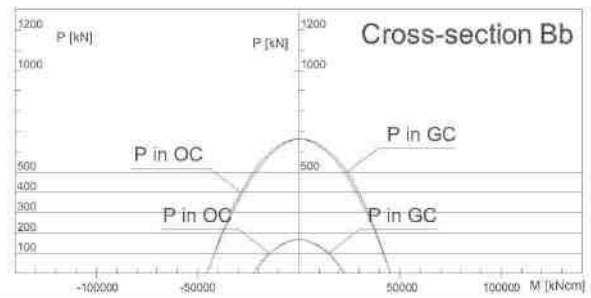


Fig. 18. Contour lines for cross-section Bb when $M_3=0$. Upper lines for simply supported beam and lower for cantilever. Moreover, longitudinal force is acting in geometrical centre (GC) or in origin of coordinates (OC).

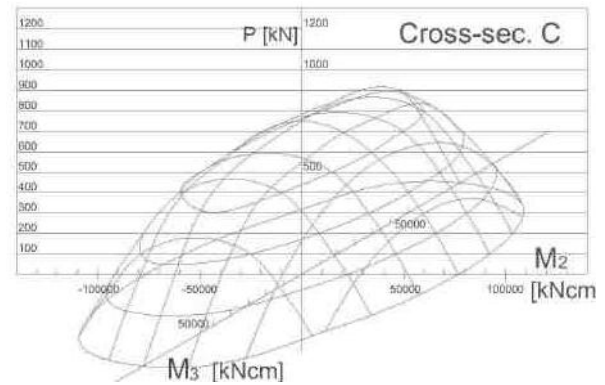


Fig. 19. Example of ultimate critical surface for combined loadings: P, M_2 and M_3 for cross-section C. Simply supported beam. Force P is acting in origin of coordinates.

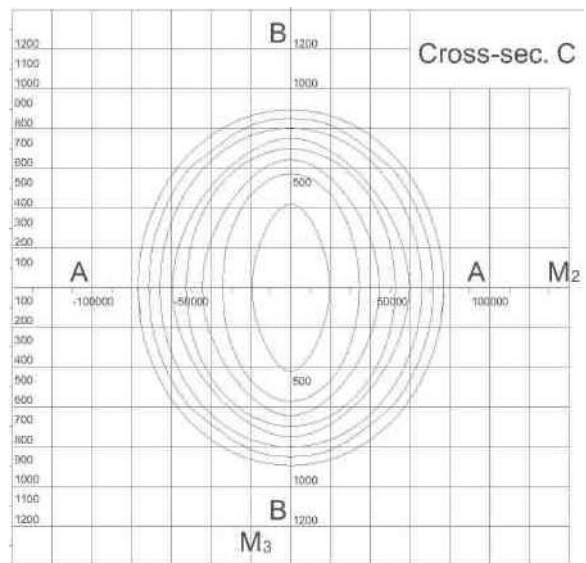


Fig. 20. Contour lines on ultimate critical surface for cross-section C and given force P, Fig. 13. Force P is acting in origin of coordinates.

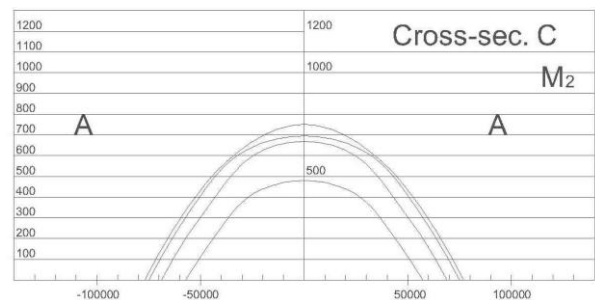


Fig. 21. Contour lines on ultimate critical surface for cross-section C and given M_3 , Fig. 13. Force P is acting in origin of coordinates.

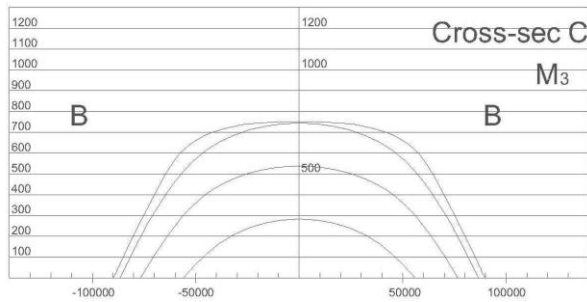


Fig. 22. Contour lines on ultimate critical surface for cross-section C for combined loadings P and M_3 and given M_2 , Fig. 13 [22]. Force P is acting in origin of coordinates.

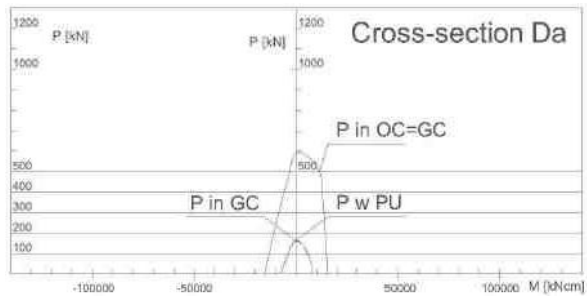


Fig. 23. Contour lines for cross-section Da and given $M_3=0$. Upper lines for simply supported beam and lower for cantilever. Moreover, longitudinal force is acting in geometrical centre (GC) or in origin of coordinates (OC).

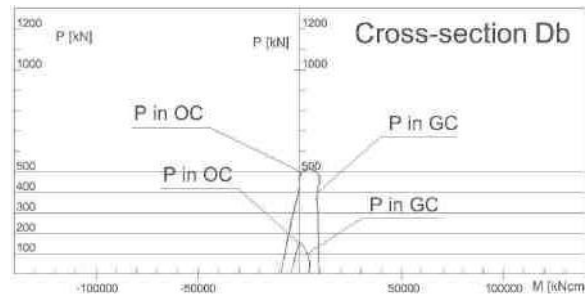


Fig. 24. Contour lines for cross-section Db and given $M_3=0$. Upper lines for simply supported beam and lower for cantilever. Moreover, longitudinal force is acting in geometrical centre (GC) or in origin of coordinates (OC).

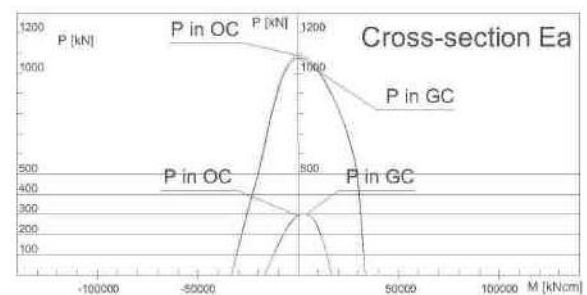


Fig. 25. Contour lines for cross-section Ea and given $M_3=0$. Upper lines for simply supported beam and lower for cantilever. Moreover, longitudinal force is acting in geometrical centre (GC) or in origin of coordinates (OC).

6.4. Comments to examples presented in chapter 6.3

Drawings from Figs 13, 15, 19, 21, 31, and 33 were published in Ref. without any formulae with short comment, only.

1. The most important conclusion of this paper is fact, that calculation of critical loadings is possible for any type of bars with all kinds of cross-sections: thin-walled of open or closed type, full and homogenous and composite.

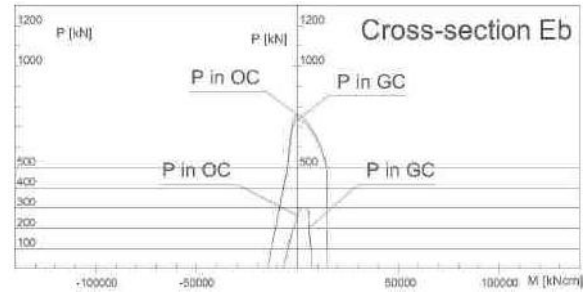


Fig. 26. Contour lines for cross-section Eb and given $M_3=0$. Upper lines for simply supported beam and lower for cantilever. Moreover, longitudinal force is acting in geometrical centre (GC) or in origin of coordinates (OC).

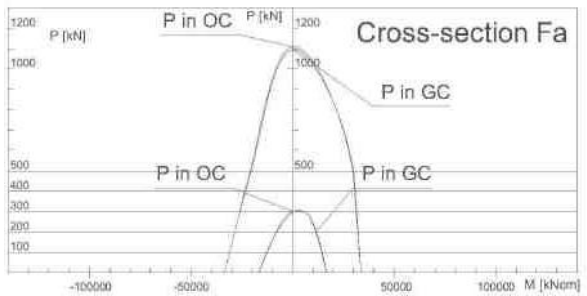


Fig. 27. Contour lines for cross-section Fa and given $M_3=0$. Upper lines for simply supported beam and lower for cantilever. Moreover, longitudinal force is acting in geometrical centre (GC) or in origin of coordinates (OC).

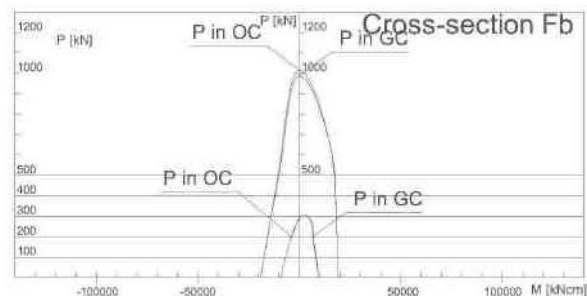


Fig. 28. Contour lines for cross-section Fb and given $M_3=0$. Upper lines for simply supported beam and lower for cantilever. Moreover, longitudinal force is acting in geometrical centre (GC) or in origin of coordinates (OC).

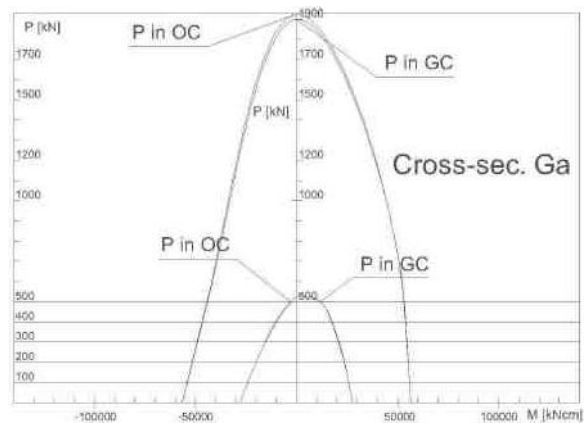


Fig. 29. Contour lines for cross-section Ga and given $M_3=0$. Upper lines for simply supported beam and lower for cantilever. Moreover, longitudinal force is acting in geometrical centre (GC) or in origin of coordinates (OC).

2. It is possible for particular bar calculation state of simple or combined critical loadings and even determination of ultimate critical curves or surfaces, and safe zones. As external loadings in this paper were used:

compressing force and bending moments. Moreover, can be solved similar tasks for transversal concentrated or continuous loadings acting in two principal planes of the bar.

3. Quoted examples shows, that instability phenomenon is in fact multiparametrical. It depends on changes of:
 - bar length,
 - bar cross-section (shape, magnitude, used materials, symmetry, bisymmetry),
 - bar boundary conditions,
 - applied external loadings,
 - position of shearing centre and positions of external loadings.
4. The bar boundary conditions can be described by declaration of three coefficients A_1, A_2, A_3 , ($A_i = (a_i)^2$, see Ref. 6, Table 9.2, page 237) given independently for each of three displacements functions (see Eqns 16). In analysed examples were taken values: 1; 4; 2,0412; 0,25.
5. Full cross-sections can be modelled as set of tubes located each into the other: homogenous or composite or also any combination of such prismatic tubes. Each division of bar cross-section on thin-walled tubes answer for other bar behaviour.
6. If we observe, that each of considered cross-sections of the Fig. 2, have other values of:
 - a) torsion rigidity K_s ,
 - b) sectorial moment of inertia \bar{I}_ω ,
 - c) position of shearing centre,

than on one of the axes we can shown e.g. one of these quantities a) to c) and this way we can obtain next type of ultimate critical curve or surface universal for certain family of cross-sections. This problem is worthy of separate study.

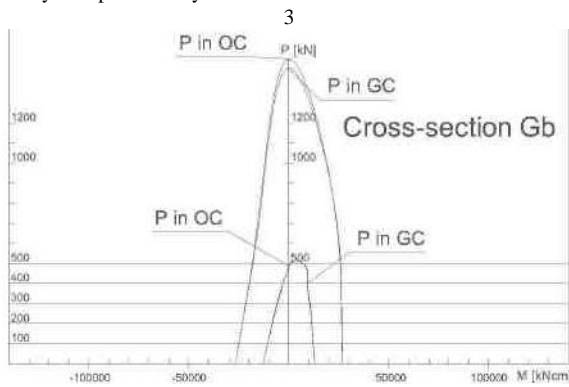


Fig. 30. Contour lines for cross-section Gb and given $M_3=0$. Upper lines for simply supported beam and lower for cantilever. Moreover, longitudinal force is acting in geometrical centre (GC) or in origin of coordinates (OC).

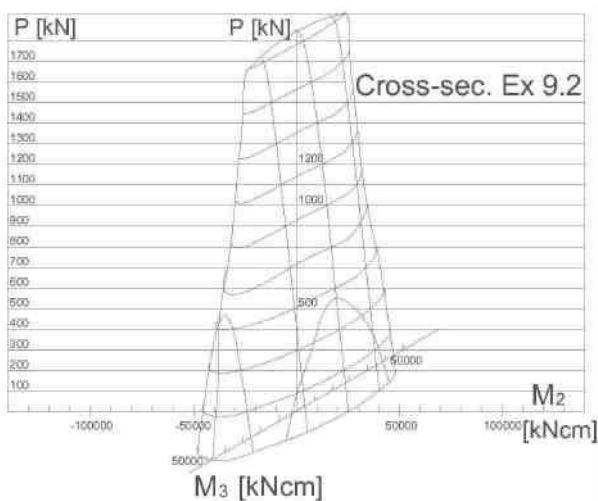


Fig. 31. Contour lines on ultimate critical surface for cross-section Ex 9.2. Simply supported beam. Force P is acting in origin of coordinates.

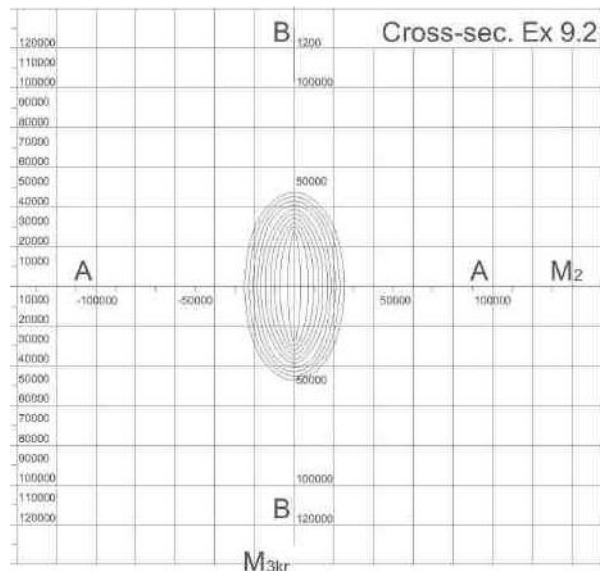


Fig. 32. Example of contour lines on ultimate critical surface for combined loadings: P, M_2 and M_3 for cross-section Ex 9.2, Fig. 31. Force P is acting in origin of coordinates.

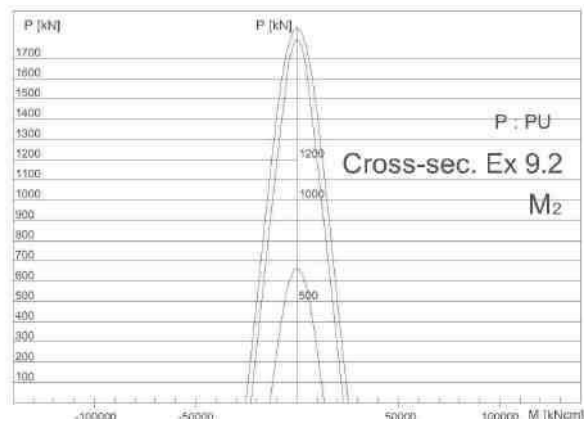


Fig. 33. Contour lines on ultimate critical surface for combined loadings P and M_2 for cross-section Ex 9.2, $M_3=0$ [22], Fig. 31. Force P is acting in origin of coordinates.

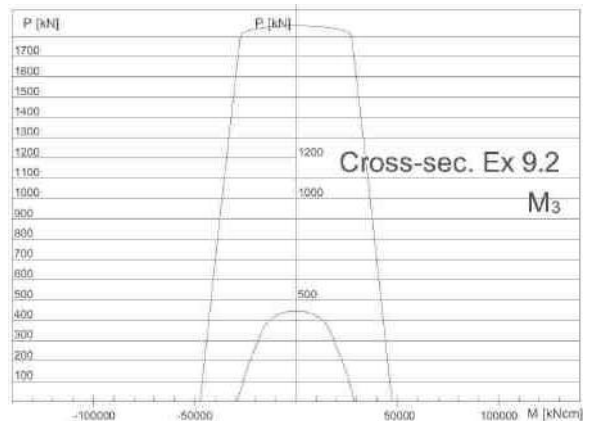


Fig. 34. Contour lines on ultimate critical surface for cross-section Ex 9.2 and given $M_2=0$, Fig. 31. Force P is acting in origin of coordinates.

7. If we look more carefully on results given in previous papers Refs. 22, 24, we can see that thin-walled cross-section assure very well behaviour of the bar, also with regard to possibility of instability, by simultaneously low material consumption. I type cross-section 59 cm^2 while, the cross-section type D has $32/88 \text{ cm}^2$ (steel/timber), type C – $40/80 \text{ cm}^2$ and type - B $60/60 \text{ cm}^2$. If we look especially on diagrams in the Figs 35, 36, it is seen that I cross-section is the best.

Similarly, cross-sections E (84/36 cm²) & F (96/24 cm²) with much higher part of steel appears much less profitable.

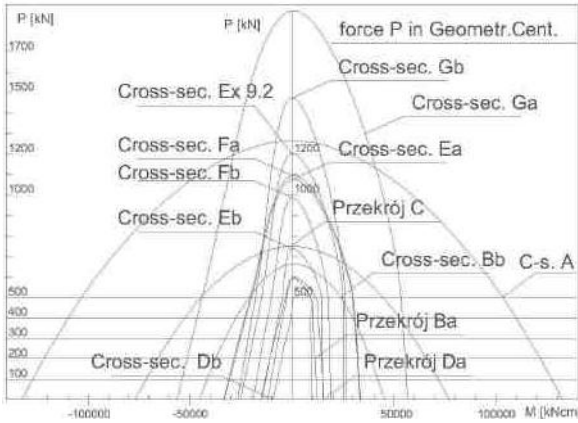


Fig. 35. Comparison of contour lines of critical surfaces for all considered cross-sections for given M_3 when force P is applied to geometrical centre. Simply supported beam.

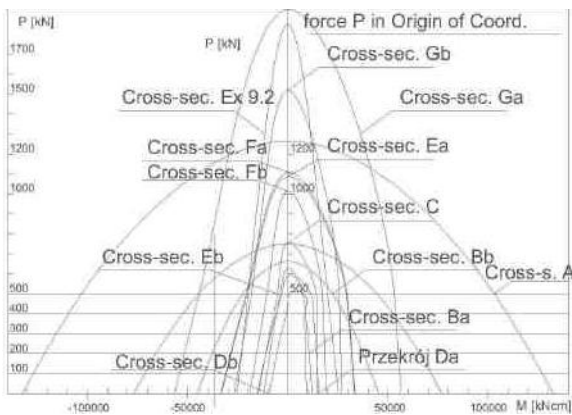


Fig. 36. Comparison of contour lines of critical surfaces for all considered cross-sections for given M_3 when force P is applied to origin of coordinates. Simply supported beam.

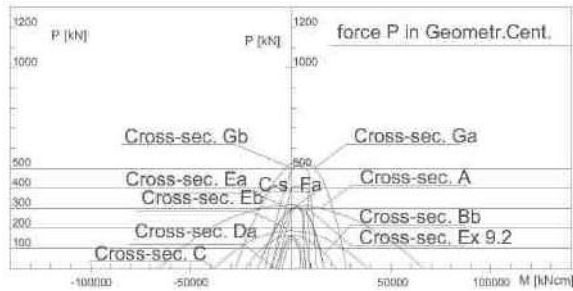


Fig. 37. Comparison of contour lines of critical surfaces for cantilever with all considered cross-sections for given M_3 when force P is applied to geometrical centre.

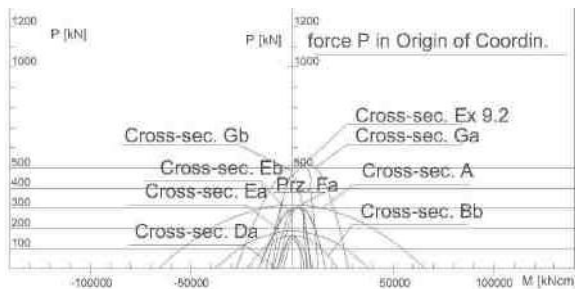


Fig. 38. Comparison of contour lines of critical surfaces for cantilever with all considered cross-sections for given M_3 when force P is applied to origin of coordinates.

6.5. Possible other states of external critical loadings

In whole chapter 6 was discussed behaviour of the bars loaded by combined loading consisting from three external forces: compressing force P and two bending moments M_2 and M_3 . In reality, Force P can act eccentrically (see Eqns 19a) and first of all used equilibrium Eqns 9 are derived for the section of the bar with length "dx", only! So shown here derived formulae can be used in some other specific tasks, what is explained shortly below.

First example, proved experimentally, concern of determination of critical bending moments for steel post with T-section, supporting acoustic screens designed for highway around city Wrocław, Poland Refs 1, 16. There analysed post have curved shape, and from assumption loaded by wind only, acting in plane of symmetry of its cross-section. There, maximal bending moment appears at down of pillar, in place of its fastening. Therefore, it were applied for solution just Eqns 9, with further derivations (see Ref. 16). In result calculated this way critical bending moment was proved experimentally in the paper Ref. 1, with practically high accuracy.

Now, we can indicate, that for simply supported bar as in Fig. 1, maximal bending moments obtain for continuous transversal loading q and for transversal concentrated loading P maximal values, relatively:

$$M_2 = \frac{ql^2}{8} \quad \text{or} \quad M_3 = \frac{Pl}{4} \quad (33)$$

Similarly, for cantilever loaded by continuous transversal loading q we have in fixed point maximal bending moment

$$M_2 = \frac{ql^2}{8} \quad (34)$$

So, if we replace in derived above formulae, given in chapter 6.2 bending moments by shown above Eqns 33 or 34, it will be possible to obtain critical states of combined loading by continuous or concentrated transversal forces.

7. APPLICATION OF FINITE DIFFERENCES METHOD

As it is shown e.g. by Obrębski in Refs 9, 12, Finite Differences Method is very useful for numerical calculation of many more complicated tasks. Solution is obtained in relatively easy manner replacing differential equations by identical, but Finite Differences Operators. Especially it is useful for determination of:

- beams deflections and internal forces,
 - critical loadings by more complicated tasks (Obrębski Ref. 13),
 - dynamical behaviour of structures, applying 3D-Time Space Method,
- for of bridge girders under moving loadings,
for tall buildings, etc.

Applying FDM, any task, which has theoretical solution in the form of differential equations, can be transformed to Finite Differences Operators (FDO), ever in the polynomial shape:

$$C_r \left(A_{ro} + \sum_{\lambda=1}^n A_{r\lambda} E_\lambda \right) \Phi_r = Q_r \quad (35)$$

where, the symbols A and C mean proper coefficients, e.g. Refs 12, 23. In result we come to solution of Eqn

$$Kx = Q \quad (36)$$

for determination of unknown displacements x of whole structure. There, unknown displacements x are determined, by given set of nodal forces Q and K – stiffness matrix of whole structure, composed by means of Eqn 35.

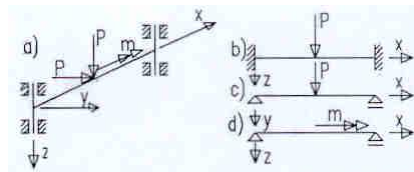


Fig. 39. Three independent schemes for displacements of single bar on some approaches, LSCE 2001, 2003 (see e.g. Ref. 23).

Equation 36 is simply set of algebraic linear equations. Composition of Eqn 36 and solution can be performed by small author's program MRS (17.5 kB). As it is explained in the Fig. 39, for one bar can be used a set of e.g. three equations (FDO), each with other boundary conditions.

7.1. Finite Differences Method in static tasks

One of the simplest examples is shown in the Figs 40 & 41, where straight bar has variable rigidity generated by different number of applied steel reinforcements (Fig. 40) located on bar length, as it explain Fig.41 with cross-sections $\gamma-\gamma$, $\delta-\delta$, $\xi-\xi$.

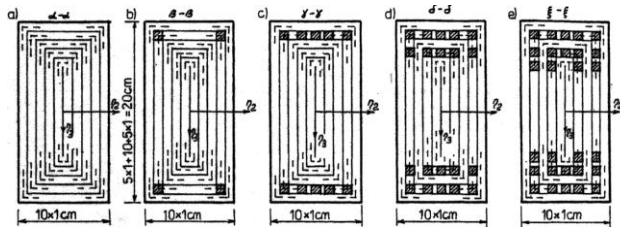


Fig. 40. Examples of reinforced cross-sections.

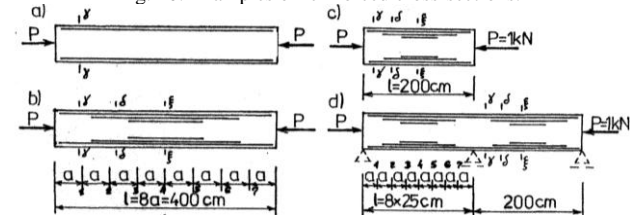


Fig. 41: Examples of reinforced bars with variable rigidity on its length.

7.2. Finite Differences in dynamics – 3D Time Space Method

Shortly the approach is named 3D-Time Space Method (or 3D-TSM). There, is introduced time as the fourth dimension. It is assumed, that motion equations of whole space structure are combined with Finite Differences Method. The method was discussed in some papers, Ref. 12, 21, 23.

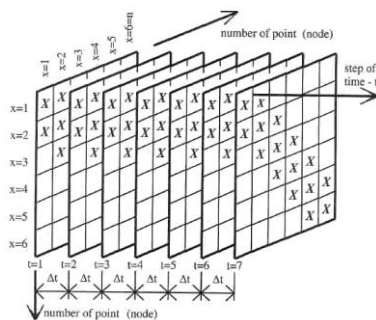


Fig. 42. Idea of the dynamical stiffness matrix, Ref. 23.

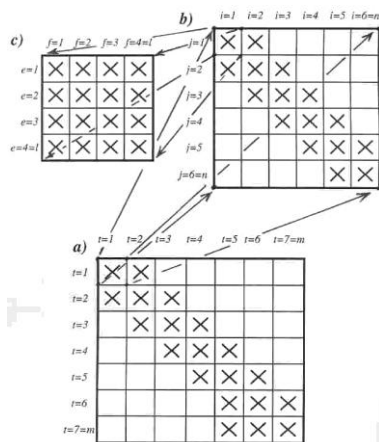


Fig. 43. Scheme of the dynamical stiffness matrix from Fig 42, applied in computer program.

It were solved some examples of application the method. Here are presented the simplest. First concern of the mass moving with velocity v along freely supported beam, Fig.44. The bar was divided on 10 sections. In the Fig.45 are shown deflected axes of the beam for all 11 considered time moments (series). Diagrams are produced by MS Excel.

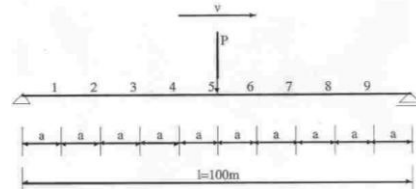


Fig. 44. Concentrated force moving along simply supported beam, with velocity v , Ref.23.

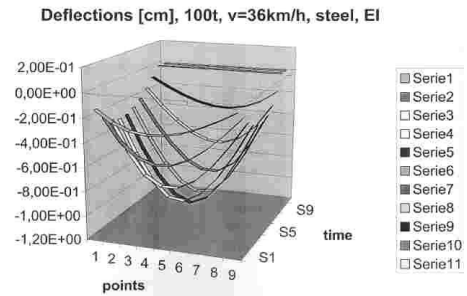


Fig. 45. Deflections of the beam from Fig 44, given in cm. Mass 100t is moving with velocity 36 km/h.

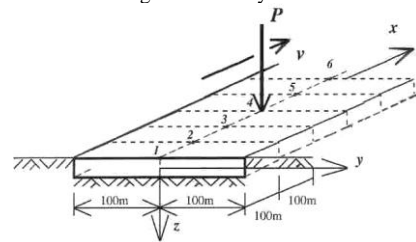


Fig. 46. Concentrated force is moving along the concrete band.

The next example shown in the Fig. 46 concern of the big aircraft moving along concrete airport landing band, located on soil. In the example, for possibly simple presentation of results, were applied not numerous division as well in 3D space as in time axis, too.

The FDM was applied for dynamical behaviour of tall buildings, too (R. Szmit, see Ref. 23), Figs 47-50.

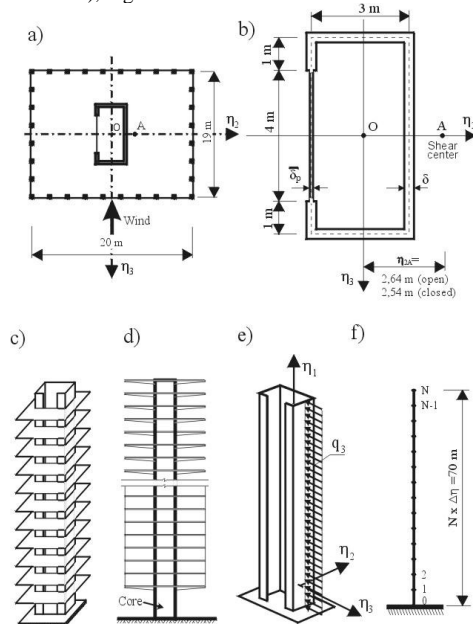


Fig. 48. Examples of cross-section and manner of modelling of the tall building as cantilever.

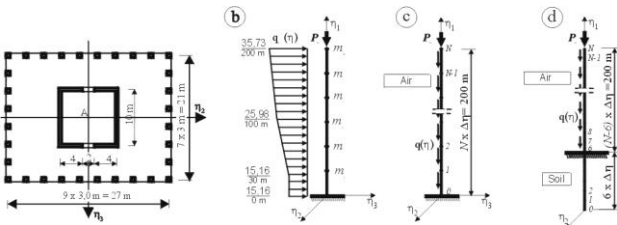


Fig. 47. Cross-section and schemes of a tall building modelled as thin-walled cantilever with two closed rectangular tubes.

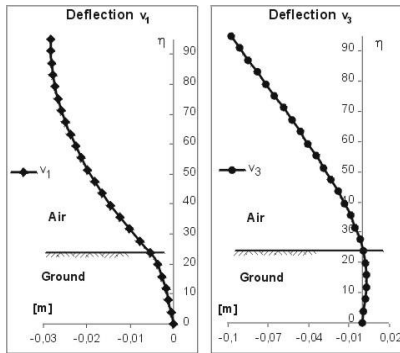


Fig. 49. Deflections of the analyzed model of the building calculated for two principal planes of the cross-section.

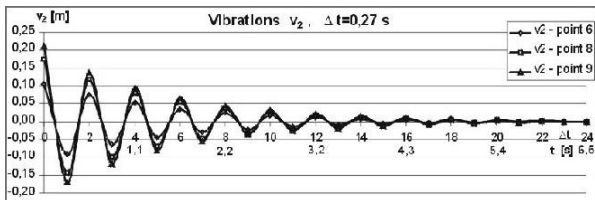


Fig. 50. Calculated oscillations of the building deflections for three its levels

8. APPLICATION OF FINITE ELEMENT METHOD

There, were elaborated two own algorithms for space bar structures by Finite Element Method application

- small program MES (name in Polish) for didactic purposes in University of Warmia and Mazury in Olsztyn,
- large program system for technical optimization of mainly space bar domes for (written and tested with A.H. Fahema) named as SPES (SPace structurES).

Program system SPES consists of some programs for:

- printing scheme of structure,
- analysis of structure,
- analysis of calculated results (searching minimal or maximal values of displacements, internal forces, stresses, geometry of structure, volume of built in material, weight of structure, comparisons of some declared tasks (up to 20) etc.

9. APPLICATION OF FINITE DIFFERENCES CALCULUS

The first author's more important solutions concern determination of internal forces in range of statics for plane regular hexagonal grids. There, was used calculus of finite differences and obtained solutions were in form of closed formulae. In this way were obtained results for: straight bars loaded in regular way; for hexagonal plane grid, which was simply supported on circular external edges, Fig. 51-54 and for infinite strips - hexagonal grid with some kinds of boundary conditions, Refs 2, 3 and Figs 55-57. In each of above solutions firstly were determined deflections of nodes, and next bending moments and shearing forces Refs 2, 3. All solutions are in the form of closed formulae.

Some possible shapes of closed edges for supports of hexagonal regular grids are shown in the Fig. 58.

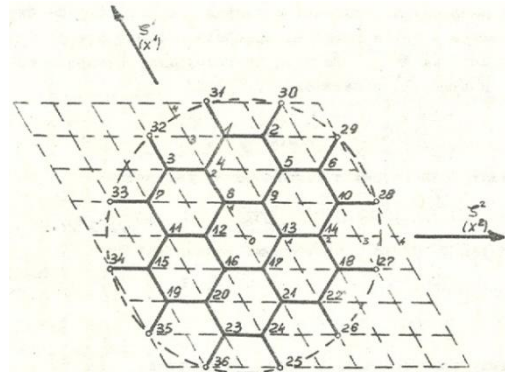


Fig. 51. Calculated hexagonal plane grid loaded in all nodes by forces P, Refs. 2, 3.

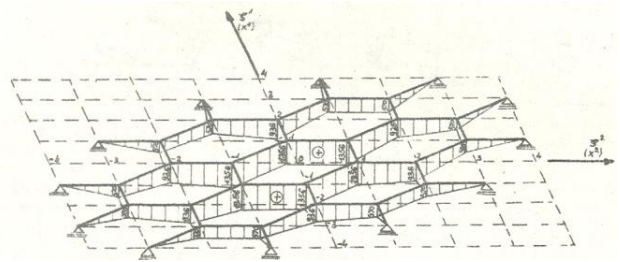


Fig. 52. Diagram of calculated deflections. Shown deflections should be multiplied by $(\pi^3)/(72EI)$, Refs 2, 3.

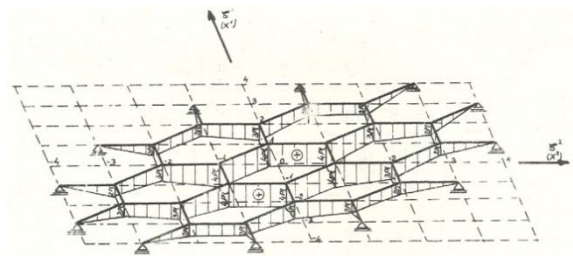


Fig. 53. Diagram of calculated bending moments, Refs 2, 3.

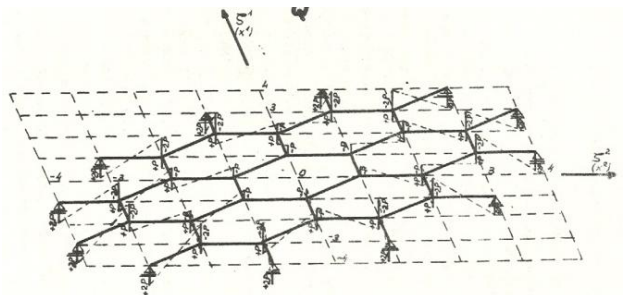


Fig. 54. Diagram of calculated shearing forces Refs 2, 3.

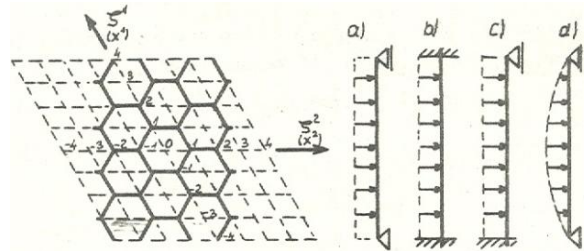


Fig. 55. Band of hexagonal plane grid and four variants of analyzed transversal loadings, Refs 2, 3.

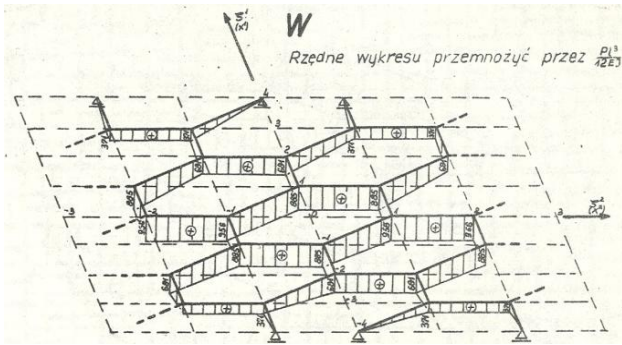


Fig. 56. Diagram of calculated deflections. Shown deflections should be multiplied by $(Pl^3)/(12EI)$ [66]

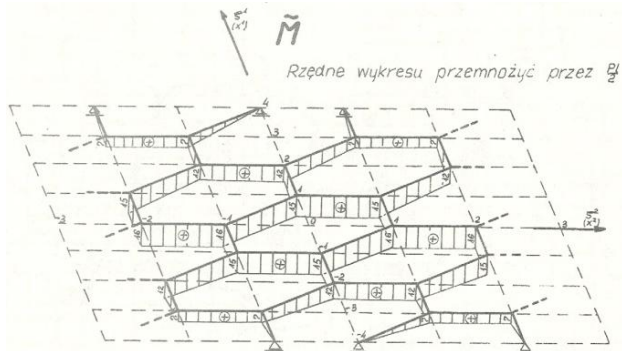


Fig. 57. Diagram of calculated bending moments. Shown values should be multiplied by $Pl/2$, Refs 2, 3.

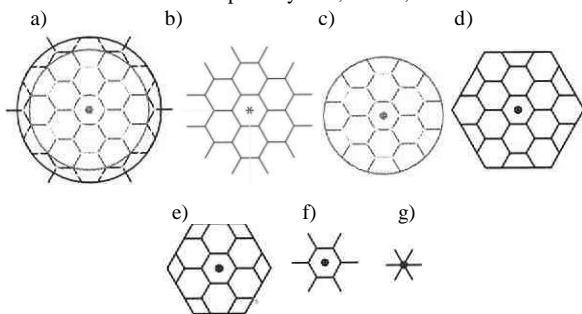


Fig. 58. The hexagonal grids b-g possible for analytical solutions

10. HYBRID METHODS OF ANALYSIS

It is important, that applying equations derived for Finite Differences Equation Method (Refs 2, 3) to the computer (hybrid method), we obtain simply set of linear algebraic equation (46). In this case structure can be much complicated and have any boundary conditions and to be loaded in each node by other force (see Ref. 23). By such approach family of structures shown in the Figs 51-58 can be much wider, not limited by necessity to fulfil in analytical way of structure boundary conditions.

11. PART OF EXPERIMENTS IN STRUCTURES ANALYSIS

The first significant experimental tests were performed on series thin-walled cantilevers under combined loading - bended eccentrically. Schemes of the experiments are shown in the Figs 59-61.

The experiments were done by the author himself and in cooperation with S. Wichniewicz, Z. Urbaniak, P. Flont. The experiments were performed mainly in years 1988-1992 and elaborated partially a little later, Ref. 23. There, were compared similar thin-walled brazen cantilevers with open or closed CSS, with thicknesses of walls $\delta = 0.5; 1.5$ and 2.5mm .

Moreover, were applied two different boundary conditions. Cantilevers at left, were fully fastened and at right were at all free end or plenary constrained by rigid still cork, Figs 77 and 78.

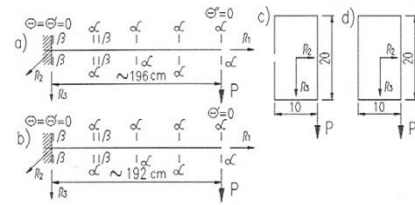


Fig. 59. Scheme of the experiment

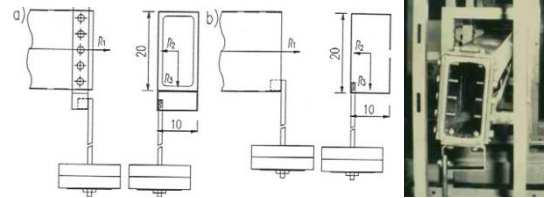


Fig. 60. Loading system for thin-walled bars (Fig.59)

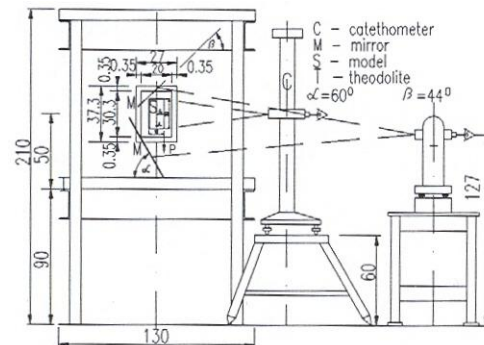


Fig. 61. Scheme of stand used by author for experiments with cantilever thin-walled bars (Fig. 59).



Fig. 62. At left different distances from fastened end of hinges (breaking point in lower part - dependently on boundary conditions) for thin-walled cantilevers (Fig. 59) and at right views from both sides.

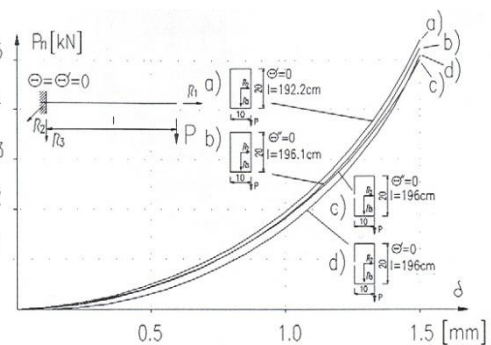
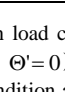
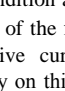
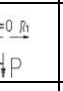
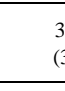


Fig. 63. Capacity P_n of the cantilevers dependently on type of CSS, applied boundary conditions and on thickness of bar walls.

As consequence of above schemes were obtained measured results of similar bars load capacity given in Table 1.

Table 1. Measured critical loadings (load carrying capacity) for cantilevers with walls thickness 0.5mm, with open or closed cross-sections, with free- or plenary constrained right end.

Scheme of the cantilever	P _n load capacity [kN] (hanging mass [kg]) by given bar cross-section δ=0.5 mm	
		
	302.858 (30.883)	430.345 (43.883)
	442.702 (45.143)	488.793 (49.843)

There, bar with open CS has obtain load capacity P_n=45.143kg, (with boundary condition at free bar end Θ'=0) higher than bar wit closed CS P_n=43.883kg (with boundary condition at free bar end Θ'=0). It is result of better boundary conditions of the first bar. Simultaneously, in the Fig. 63, are given comparative curves showing character of dependences of bar load on capacity on thickness δ of its walls. It is strongly nonlinear. We can draw conclusion, that **by thicker bar walls, influence of local instability is much smaller**. Some more interesting results are shown in the Figs 82-86.

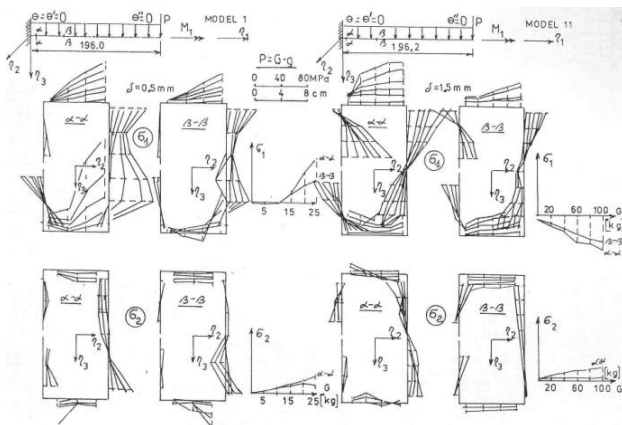


Fig. 64. Calculated normal stresses: longitudinal and circular; in two different (open type) CSs α-α and b-b in distance from fastening relatively 2 cm and 55 cm, Figs 59, 60; thickness of bar walls δ=0.5 mm and δ=1.5mm. The right end of cantilever at all free.

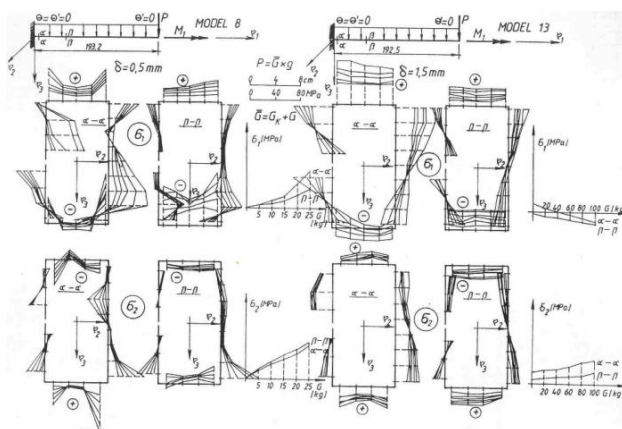


Fig. 65. Calculated normal stresses: longitudinal and circular; in two different (open type) CSs α-α and b-b in distance from fastening relatively 2 cm and 55 cm, Figs 59, 60; thickness of bar walls δ=0.5 mm and δ=1.5mm. The right end of cantilever plenary constrained by rigid steel cork (see Fig. 60).

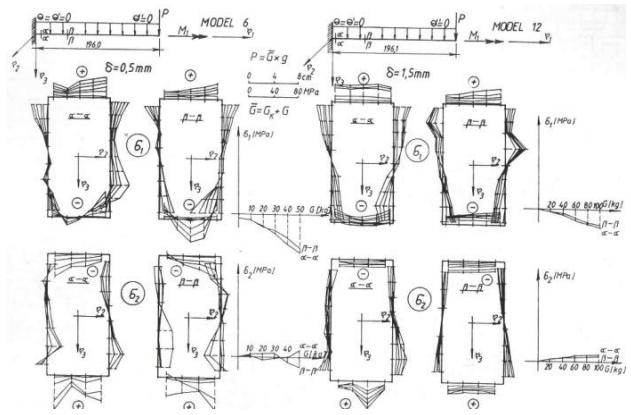


Fig. 66. Calculated normal stresses: longitudinal and circular; in two different (closed type) CSs α-α and b-b in distance from fastening relatively 2 cm and 55 cm, Figs 59, 60; thickness of bar walls δ=0.5 mm and δ=1.5mm. The right end of cantilever at all free.

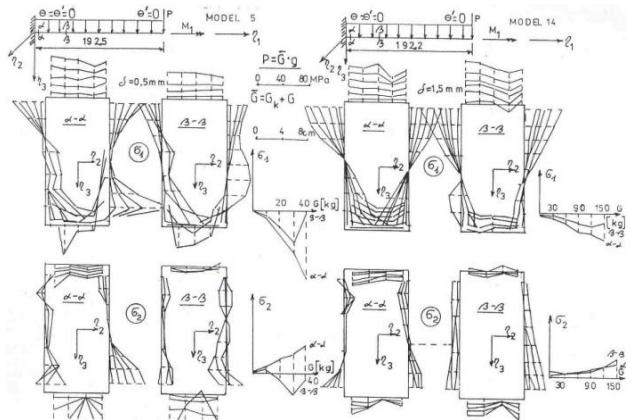


Fig. 67. Calculated normal stresses: longitudinal and circular; in two different (closed type) CSs α-α and b-b in distance from fastening relatively 2 cm and 55 cm, Figs 59,60; thickness of bar walls δ=0.5 mm and δ=1.5mm. The right end of cantilever plenary constrained by rigid steel cork (see Fig. 60).

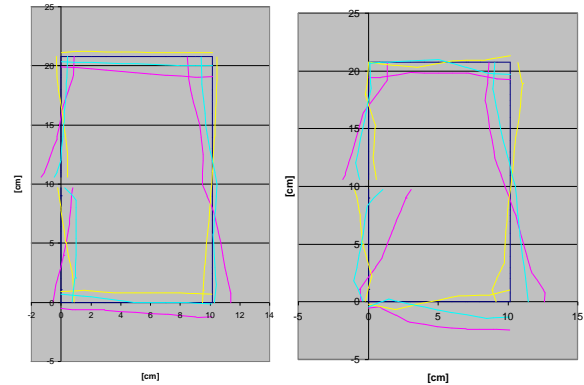


Fig. 68. Diagrams of measured strains for model No 11 with walls thickness app. δ=1.5 mm by hanging mass 100 kg in CSs α-α (2 cm from fastening) and b-b (55cm from fastening), Fig. 59. Black lines – shape of CS, redlines – longitudinal strains, yellow lines – circular strains, green lines – inclined (45°) strains.

It is worthy to explain, that after electro-resistance measurements of strains (cantilevers from Fig. 59), were calculated normal σ and τ shearing stresses, which applied in Eqns (26) permits to determinate of measured bimoments B and bending-torsion moments, given in Table 2 (J.B. Obrębski, Ref. 23). The bimoment and bending-torsion moment have among the others, two following definitions:

$$B = \int \sigma_i \omega dA = \int \sigma \alpha ds, \quad M_\omega = \int \tau n ds, \quad (26)$$

expressed by: stream of normal stresses σ or shearing stresses τ and its arm n.

It should be added, that shearing and normal stresses occurring in Eqns (26) can be experimentally measured, or calculated by any method, e.g. by FEM. This idea was used in Ph.D. dissertation of N. Jankowska, Ref. 23. Such calculations are much better for open type CSs, where investigated forces are much higher.

Table 2. Internal forces - bimoments and bending-torsion moments calculated analytically accordingly to Eqns 26 (method proposed by J.B.Obrębski using measured experimentally σ and τ , Fig.77).

Internal Force	Model 21 with open cross-section		Model 22 with closed cross-section	
	analytical	measured	analytical	Measured
B [kNcm ²]	831.82	848.475	-4.826	9.65
M _ω [kNcm]	-10.1908	-2.175	2.189	3.35

11.1. Experimental estimation of critical bimoment

Together with M.E. El Awadi from Egypt (1992, see Ref. 23), were executed relatively simple experiments for confirmation of possibility to appear of critical bimoment - instability effects by loading bar by pure bimoment – derived theoretically Ref. 9.

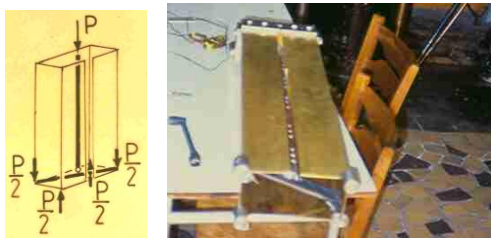


Fig. 87. Scheme of loading applied to model and its photo.

Scheme of experiment is shown in the Fig. 87. As critical bimoment calculated as effect of force P, was noted moment of appearance of waves on longitudinal edges of the slit, Fig. 88. The diagrams in the Fig. 89 shows comparisons of measured experimentally and calculated theoretically, critical bimoments. For thin walls of model both results are almost identical.

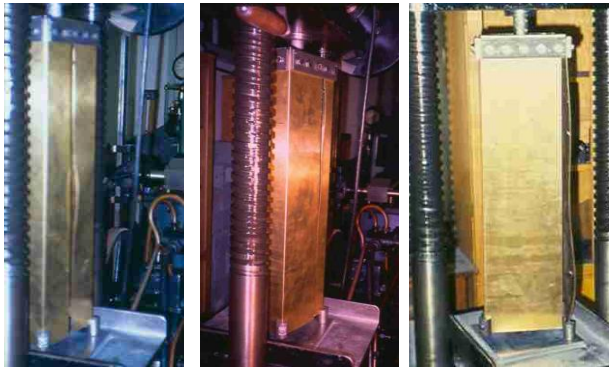


Fig. 88. Three different models loaded by pure bimoment (see Fig. 87) with visible waves on free longitudinal slits.

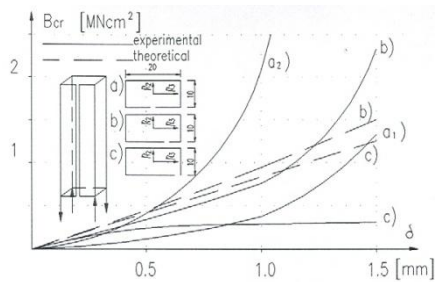


Fig. 89. Observed and theoretically calculated [86] critical bimoment measured with M.E.El Awadi (Egypt) dependently on thickness of bar walls and applied bar cross-section

Similarly, the special attention was there focused on some visible bimoment influence on instability for mentioned above thin-walled cantilevers. Shown photographs and drawings (e.g. Figs 78, 80-85) presents observed effects. In the light of these experiments, the bimoment is evidently the real internal force, very dangerous for structures, which should be seriously considered by designing of objects composed from thin-walled bars.

11.2. Experimental investigation of thin-walled nodes under torsion

Author has turned attention also on transmission of torsion forces (bimoment and bending-torsion moment) through plane nodes connecting 2 or 3 thin-walled bars, Figs 90-92. These experiments were performed by N.Jankowska as Ph.D. work (see Ref. 23) proposed and supervised by author.



Fig. 90. View on whole model of Y2 type (node walls is 2 times thicker than bars).

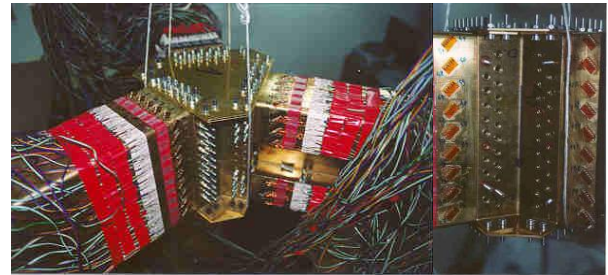


Fig. 91. Electro-resistance measuring equipments for model with node type Y2.

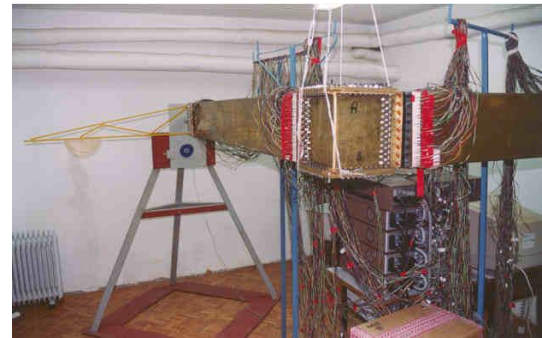


Fig. 92. Electro-resistance measuring equipments for model with node type L. Visible scanners, loading system, and location of sensors (rosettes).

Table 3. Measured bimoments (N. Jankowska see Ref 23)

i – number of sheets in central node	Frame type Li			Frame type Ti			Frame Yi	
	1	2	3	1	2	3	Y1	Y2
C –active CS	-1364	-1355	-1259	-1495	-1390	-1339	-1413	-1333
B-passive CS	-455			-285	-261	-241	-322	-285
E-passive CS				287	244	222	259	223

In the Table 3 are given condensed results of investigations by N.Jankowska transmission of torsion forces (bimoment) from active (C)

to passive (B, E) cross-sections through plane nodes connecting 2 or 3 thin-walled bars.

11.3. Experiments for presentation during lectures

The last series of simple author's experiments were planned for didactic purposes, to be presented for students during lectures on slides. It permits to show, that calculated phenomena can be simply observed...



Fig. 93. The photo of warping on torsioned much box – identical as calculated analytically by theory, Refs 6, 9.

Such presentations during lecture, as shown in the Figs 93-97 (LSCE 2009) makes theory much easy for understanding, its necessity, existing warping as effect of torsion and at last, appearing warping stresses.

In many cases for proving certain, real behaviour of structure is enough very simple, not expensive, but well thought out strategy of performed experiment.

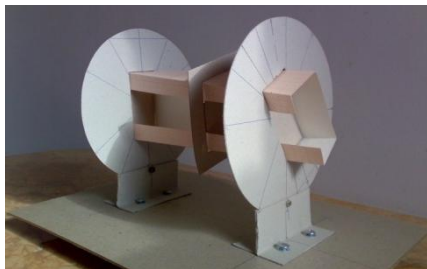


Fig. 94. Torsioned cartoon model with lipped channel cross-section.

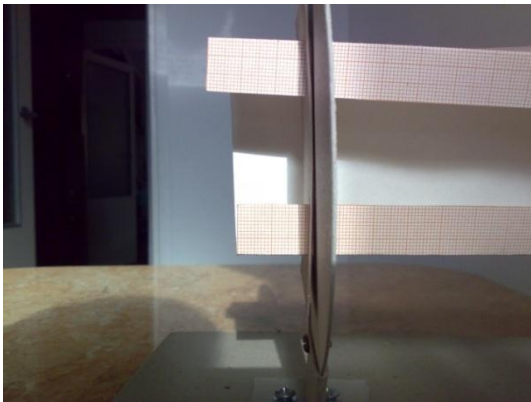


Fig. 95. Closing up for torsioned cartoon model with lipped channel cross-section.

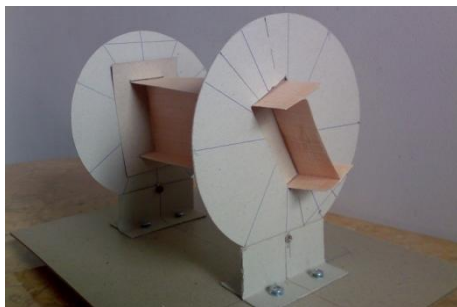


Fig. 96. Torsioned cartoon model with I cross-section, see Fig. 97.

There, are demonstrated during lectures many other simple experiments showing deflections of bars under loading, instability phenomena,

influence of boundary conditions etc. These experiments are demonstrated on objects universally used every day by peoples.

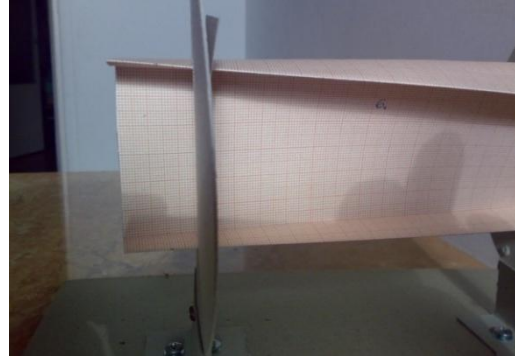


Fig. 97. Torsioned cartoon model with I cross-section; closing up.

11.4. Lessons drawn from experiments quoted in literature

Moreover, the author turns attention on experiments which can be found in literature (for details and literature see Refs 12, 21). So, in some papers and during lectures, they are quoted and compared with theory. Such results of investigations were presented in classical book of W.Z. Własow, next by A.I. Strielbitska and G.I. Jewsiejenko, and the others including done much later by A.Glinicka where were compared her experiments with FEM calculations. As extremely important, the author regard test of steel pillar instability, ordered by W. Bober, done theoretically by J.B. Obrębski and compared with experiment performed in Wrocław, (see Refs 1, 16). There, in both cases were obtained 7% of difference results.

Presentation of such comparisons during lectures and on scientific conferences permit to evaluate correctness of calculation many tasks by widely applied theories and numerical programs based e.g. on Finite Element Method (B.S. Smith, and R.P. Pruki with P.M. Lopez Cape Town 2001, A. Glinicka and J.B. Obrębski). There, FEM results seems to be very approximate – rough with errors often up to 300% and even 700% (noted by W. Szczepiński).

11.5. Full scale experiment for instability of cantilever

Next, very important analytical test was done (sent at February 10, 2010) on official order of (now) prof. W.Bober (27.11.2009), to calculate critical loading of steel pilar supporting acoustic screen for highway around Wrocław, Poland (Polish patent: by W.Bober, P.Ogielski, R.Tarczewski, K.Janczura) Ref. 1, 16. Project was managed by R.Tarczewski After theoretical calculations, by J.B.Obrębski, was determined critical bending moment. After some weeks, prof. W.Bober has sent information, that very close result was obtained experimentally. So, theory of bar instability under transversal loading generated by wind, giving critical bending moment, was excellently verified.

12. ACCURACY OF CALCULATIONS

The first wider worldwide information on menace of thin-walled structures by defects was given by author in Singapore, (see Ref. 21). But after publication of Lopez & Pruki on SEMC conference in Cape Town (2001) the author has focus his attention on many aspects of structure modelling. So, it was discussed e.g. in some author's papers (see Refs. 12, 21, 23). There, attention is turned on many matters having influence on exactness of obtained results:

- applied theory,
- applied computer method of calculation,
- structural solutions of particular bars,
- scheme of structure including structure of nodes and applied supporting system,
- exactness of Finite Element Method compared with experimental results,
- efficiency of some covering systems applied for roof structures.

13. SPACE BAR STRUCTURES - THEORY AND PROGRAMS

The first author's field of scientific activity was analysis of complicated space bar structures. Small part of beginning these investigations is

presented in the Refs 2-4. More advanced elements of elaborated theory, examples and particular references are given in reviewing papers Refs 12, 20, 21, 23. For introducing here some more interesting author's results, below are shown some computer drawings without any further comments.

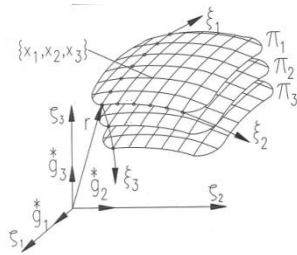


Fig. 98. Definition of net of points, used for structures from Figs 99-102, Ref. 3.

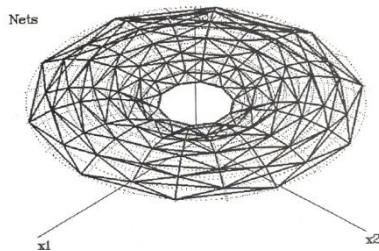


Fig. 99. Structure spread on toroidal net of points, Obrębski Bulletin of IASS v.36, 1995, n. 2 August.

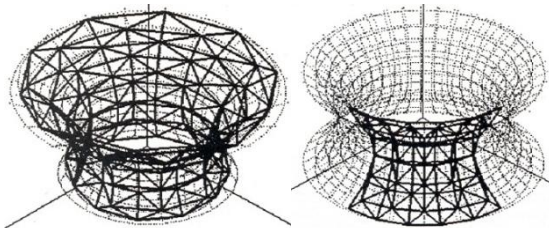


Fig. 100. Two next double-layer structures spread on toroidal net of points, Obrębski Bulletin of IASS v.36, 1995, n. 2 August.

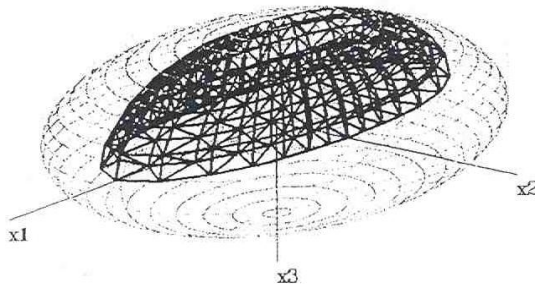


Fig. 101. Elliptical structure, program elaborated for Ph.D. dissertation of A.H. Fahema (Libya).

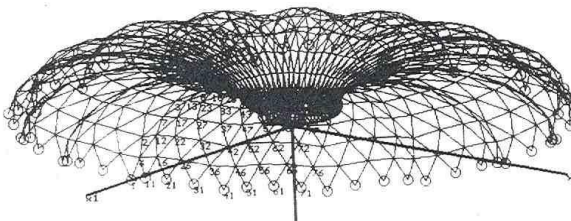


Fig. 102. Structure wavy vertically and horizontally, program elaborated for Ph.D. dissertation of A.H. Fahema (Libya).

For analysis of all above structures were elaborated proper programs based on theory initially formulated in Ref. 3.

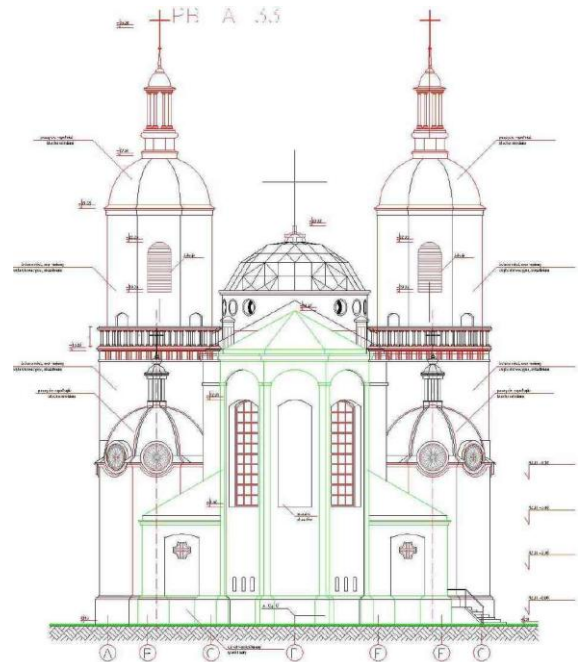


Fig. 103. Project of church with visible UNIDOM type skylight and four masonry ribbed domes – original author's structures, Ref. 23.

14. CONCLUSIONS

During more than twenty last years, on the ground of unconventional theory elaborated by present author, step by step were solved different tasks and examples, non typical for traditional strength of materials and for structural mechanics, too. On basis of these results it was possible to formulate in previous authors works many important observations and conclusions. Below are quoted some more interesting and especially new.

1. For bars with full and even composite cross-sections, are possible strength and mechanical analyses, identical as for thin-walled bars, in full range of theory for thin-walled bars (Obrębski, Refs 17-25).
2. Shown in chapter 6 application of uniform criterion to instability problems, even by combined loadings can be much more complicated, exact and very efficient than up to now (Obrębski Refs 16, 21-25 & with Tolksdorf Refs 10, 11).
3. All above calculations shows, that instability of the bar is much more complicated as it is in the (5). It depends on: the length of the bar, its boundary conditions, shape of cross-section, disposition and properties of materials forming cross-section (in effects position of reduced centre of gravity and shearing centre), rigidity of the bar on its length, applied external combined loadings: concentrated, continuous, eccentric, moments, longitudinal, transversal in two principal planed etc. At last it can be determined critical value of velocity and acceleration of loading or concentrated masses moving along certain bridge girder (Obrębski & with Szmít, see Refs 12, 13, 15, 16, 20-25).
4. Presented here theory elaborated by Obrębski Ref. 6, 16 was efficiently proved experimentally by Bober & Tarczewski, Ref. 1.
5. Modelling of the bars with full cross-section including even composite by means of set thin-walled bars – closed tubes or of open type, located one into the other, permit on easy way to calculate some auxiliary quantities important for strength analyses known up to now in theory of thin-walled bars: sectorial coordinates (warping function), shearing centre, torsion rigidity (with good accuracy!), internal forces – bimoment and bending-torsion moment and cross-section core etc.
6. Modelling of bars with full cross-sections, as set of thin-walled bars located one into the other, can be done on many manners. So, shown in the paper modelling as set of closed tubes, can be extended on the thin-walled bars with open cross-sections. Each choice answers of other structural solution and mechanical behaviour of the bar.
7. The most time-consuming stage of calculations for composite bars is determination of geometrical characteristics of their cross-section

associated with bar torsion. Just its knowledge permit on many new analyzes applied up to the moment for thin-walled bars, only.

8. All calculations in range of strength for discussed bars shown in some previous papers, Refs 13-25 and in this work, nowadays, after first elaboration of proper sheets of Excel, are easy for duplicate and modification. In result, e.g. in present work was possible to show results for 104 examples.
9. New, proposed analyses of bars with full cross-sections, including composite ones, gives radically new qualities of results in range of its strength.
10. Given examples show influence of change of sign for bending moments on stresses and critical loadings. Up to now it was not investigated this problem for longitudinal force P, what means critical tension for the bar, as it was shown by Własow, Mutermilch and in Refs 6, 9. It is at all real.
11. Knowledge of ultimate critical curves and surfaces for combined loadings, much significantly facilitate decisions by designing of structures.
12. Presented now results confirm conclusions from last authors papers, that process of analyses of structures having composite elements should be much advanced than it is proposed in contemporary: classical strength of materials and structural mechanics, academic lecture notes and first of all in standards. It concern not only determination of geometrical characteristics, internal forces and sectorial stresses generated by torsion, but states of combined critical loadings, too. The last problem appears as very complicated, multi-parametrical and sensitive on many structural details, what in general is not understood.
13. Here, the author can add own observations and not only, that modelling discussed here bars by means of FEM also gives not exact solutions, often very far from experimental results.
14. Summarizing, it should be suggested, that proposed here methods of strength analyses, led by aid of computer, should be introduced to normal designing practice.

14. REFERENCES

1. W. Bober, R. Tarczewski: Shaping of T-section steel post for acoustic screen Lightweight Structures in Civil Engineering - Contemporary problems. XVI Internat. Seminar of IASS Polish Chapter, Warsaw, Dec.3, 2010; Micro-Publisher J.B.O. Wydawnictwo Naukowe, pp. 97-99.
2. J.B. Obrębski: Statyka heksagonalnych siatek prętowych, (Statics of Hexagonal Bar Nets). IBTP Reports 36/1972, Warsaw, (doctor thesis).
3. J.B. Obrębski: Analiza i synteza numeryczna wielkich układów konstrukcyjnych, (Numerical Analysis and Synthesis of Large Structural Systems). IBTP Reports 24/1979, Warsaw (habilitation thesis) str. 196
4. W. Gutkowski, J.B. Obrębski, J. Bauer, J. Gierliński, J. Rączka, K. Żmijewski: Statische Berechnung der Raumstabwerke. Werner Verlag/Arkady, Warszawa, 1985. (Translation of the book: Obliczenia statyczne przekryć strukturalnych, (Statical Computations of Structural Roofs). ARKADY, Warszawa, 1980.) cooperation with publisher - J.B. Obrębski). 6-th chapter =50,2% written by J.B. Obrębski..
5. Obrębski J.B., Second-order and second-approximation theory in the statics and dynamics of thin-walled straight bars. *International Journal Thin-Walled Structures*, 1989, **8**, 81-97.
6. J.B. Obrębski: *Thin-Walled Elastic Straight Bars*, (In Polish - *Cienkościenne sprężyste pręty proste*), WPW. Warsaw 1991, pp. 452. (2nd Ed.), Oficyna Wydawnicza Politechniki Warszawskiej, Warsaw 1999; pp. 455.
7. J.B. Obrębski: Some torsion problems in thin-walled bars mechanics, Intern. Conf. Faculty of Civil Eng. Warsaw Univ. of Techn, LSCE'95, 25-29.09.1995. MAGAT, Warsaw 1995; 395-404.
8. J.B. Obrębski: Uniform criterion for geometrical unchangeability and for instability of structures. Proc. of the Intern. Conf. on Stability of Struct. Zakopane, Poland, 1997.
9. J.B. Obrębski: Strength of Materials, (In Polish – Wytrzymałość Materiałów, lecture notes), Micro-Publisher J.B.O. Wydawnictwo Naukowe, Printed by AGAT, Warsaw 1997, pp. 238.
10. J.B. Obrębski, J. Tolksdorf: Advanced examples of strength analysis for composite straight bars, in Internat. Seminar (Ukrainian-Polish), Faculty of Civil Engineering Warsaw University of Techn. &

Prydnieprovsk State Academy of Civil Engineering and Architecture, Warsaw, 2006, OWPW; 265-282.

11. J.B. Obrębski, J. Tolksdorf: Comparative examples of instability analyses for straight bars in the light of theory and standards, in *Lightweight Structures in Civil Engin. – Contemp. probl. XII Intern. Colloquium of IASS Polish Chapter*, Warsaw, Dec.1, 2006, pp.188. Micro-Publisher J.B.O., Wydawn. Naukowe; 95-112.
12. J.B. Obrębski: Review of own complex researches related to bar structures. XIV LSCE - Lightweight Structures in Civil Engineering - Contemporary Problems, Local Seminar of IASS Polish Chapter, Warsaw, 5 December, 2008, pp.87-128.
13. J.B. Obrębski: Multi Parametrical Instability of Straight Bars, Proc. of IASS-IACM the 6th Intern. Conf. on Computation of Shell and Spatial Struct. Cornell University, Ithaca, USA 28-31 May (2008)
14. J.B. Obrębski: Metody analizy prętów cienkościennych wspomagane komputerem i ich ocena WAT 2009, XIII Międzynarodowa Szkoła Komputerowego Wspomagania Projektowania, Wytwarzania i Eksploatacji, Jurata, 11-15 maja, 2009, str. 239-254.
15. J.B. Obrębski: Theory for thin-walled bars – performed investigations and tests. LSCE 2009. XV LSCE - Lightweight Structures in Civil Engineering - Contemporary Problems, International Seminar of IASS Polish Chapter, Warsaw, 4-5 December, 2009, pp. 124-143.
16. J.B. Obrębski: Stability of steel pillar supporting acoustic screen. Proc. Lightweight Struct. in Civil Engin. - Contemporary probl. XVI Intern. Semin. of IASS Polish Chapter, Warsaw, Dec.3, 2010, pp.111. Ed. by Micro-Publisher Jan B. Obrębski, Wydawn. Nauk., pp. 70-75.
17. J.B. Obrębski: Przykłady obliczania naprężeń w prętach kompozytowych przy wytrzymałości złożonej (Examples of stresses calculation for composite bars being under combined loading). WAT 2012, XVI Międzynarodowa Szkoła komputerowego wspomagania projektowania, wytwarzania i eksploatacji, Jurata 14-18.05.2012, t.2, s.61-74 & Mechanik, 7, 2012, p. 602 +CD.
18. J.B. Obrębski: Some observations on mechanical behaviour of bars with composite cross-sections. Proc. Lightweight Structures in Civil Engineering - Contemporary problems. XVIII International Seminar of IASS Polish Chapter, Warsaw, Dec.7, 2012, pp.183. Edited by Micro-Publisher Jan B. Obrębski, Wydawnictwo Naukowe, pp. 110-121.
19. J.B. Obrębski: Influence of torsion on stresses calculated for series of composite bars (Wpływ skręcania na naprężenia obliczone dla serii belek kompozytowych). (General lecture 30min) WAT 2013, XVII Międzynarodowa Szkoła Komputerowego Wspomagania Projektowania, Wytwarzania i Eksploatacji, Szczyrk, 13-17.05.2013, tom 2, pp. 77-93 & Mechanik, 7, 2013, p.598 + CD.
20. J.B. Obrębski: Behavior of composite bar structures: Theory and examples. (Invited paper 30min.) Int. Conf SEMC 2013, 2-4.09.2013, Edited by A. Zingoni, Cape Town, South Africa, CRC Press/Balkema Book, pp. 305-306 + CD.
21. J.B. Obrębski. Own impact to shaping and analyses of lightweight structures. IASS Symposium 23-27.09.2013, Wrocław, Poland, CD paper 1218, 26 pp.
22. J.B. Obrębski: Comparison of some critical loadings for simingly similar bars with composite cross-sections. XIX LSCE - Lightweight Struct. in Civil Engin. - Contemporary Problems, Local Sem. of IASS Polish Chapter, 6 Dec. 2013, Olsztyn, 6.12.2013, pp. 110-121.
23. J.B. Obrębski: Own papers published in LSCE books 1995-2012. Edited by Jan B. Obrębski. MP CP JBO Wydawnictwo Naukowe + Studio Bud., Warszawa, 2013. Monograph, pp. 632.
24. J.B. Obrębski: Examples of multi-parametrical instability of straight bars. WAT 2014, Szczyrk, 12-16.05.2014, pp. 125-142 & Mechanik, 7, 2014, p.562 + CD full paper;
25. J.B. Obrębski: Review of possible new qualities in mechanics of straight bars. IASS-SLTE Symposium, Brazil, 15-19.09.2014.

¹⁾ J.B. Obrębski, Institute of Structural Mechanics, Warsaw University of Technology, Al. Armii Ludowej 16, 00-637 Warsaw, POLAND.

tel: +48-601-82-72-87 or (4822) 845-18-85 or (4822) 825-69-85

e-mail: jobrebski@poczta.onet.pl or (SMS): (GSM) +48601827287 or fax: (4822) 845-18-85 or (48-22) 825-69-85